

Chapter 2

Evolution of Periodic Orbits in the Sun–Saturn System

2.1 Introduction

The study of periodic orbits plays an important role in the understanding of the general properties of different dynamical systems. A large number of periodic orbits were generated by [Broucke (1968)] in the framework of RTBP using numerical techniques. [Abouelmagd (2013)] has studied RTBP by including all types of perturbations. He had considered the case where both primaries are source of radiation and both primaries and secondary body are oblate spheroids and developed the equations of motion for two and three dimensional cases with perturbation due to Coriolis and centrifugal forces. He has also identified the location of equilibrium points. The study of quasi-periodic orbits is important due to its application in space mission. One way of reducing fuel consumption is to place the spacecrafts on quasi-periodic orbits, thus maintaining a maximum separation. Consequently, a number of investigations have been made for finding the quasi-periodic orbits around the libration points.

Poincaré surface of section (PSS) [Poincare (1892)] is widely used for analysing periodic, quasi-periodic and chaotic orbits. [Murray and Dermot (1999)] have given a detailed analysis of periodic orbits using PSS. Chaotic behaviour of bodies can also be studied using PSS, Liapunov characteristic numbers, Fourier transform tech-

niques and numerical irreversibility technique. The set of stable periodic and quasi-periodic trajectories define regions of regular motion or stability *islands* that spread in a chaotic *sea* made up of trajectories with high sensitivity with respect to the initial condition. As per Kolmogorov–Arnold–Moser (KAM) theory, each point of PSS represents a periodic orbit in the rotating frame, and the closed curves or *islands* around the point correspond to the quasi-periodic orbits.

PSS gives a qualitative picture of stability regions in the planar RTBP problems. [Kolmen et. al.(2007)] have employed multiple PSS method to find quasi-periodic orbits around the libration points L_1 and L_2 in the Sun–Earth system. [Winter (2000)] has studied the location and stability of periodic and quasi-periodic orbits in the Earth–Moon system. [Dutt and Sharma (2010)] and [Dutt and Sharma (2011a)] have analyzed the PSS for Earth–Moon system and Sun–Mars system. They have identified periodic, quasi-periodic solutions and chaotic regions. [Safiya Beevi and Sharma (2011)] and [Safiya Beevi (2012)] have also studied PSS for Saturn–Titan system for periodic orbits, quasi-periodic orbits and chaotic orbits.

In this chapter, PSS for different values of Jacobi constant C for perturbed Sun–Saturn system are obtained and studied the effect of C and mass reduction factor q on PSS. Also, effect of perturbation like C and q are studied on periodic and quasi-periodic orbits of secondary body of photo-gravitational Sun–Saturn system incorporating actual oblateness of Saturn in the planar CRTBP. This work is mainly concentrated on two major islands, one gives Sun centered periodic orbits and other gives Saturn centered periodic orbits. Since these two islands are major islands they are available in each PSS corresponding to different solar radiation pressure q with different Jacobi constant C . So, effect of perturbation on the geometrical parameters of two different families of periodic orbits, like location of Sun centered and Saturn centered orbits, its diameter, semi major axis and eccentricity are analyzed.

2.2 Computational technique

For the Sun–Saturn system, mass of the Sun is $m_1 = 1.9881 \times 10^{30}$ kg and mass of Saturn is $m_2 = 5.6836 \times 10^{26}$ kg. Thus, $\mu = \frac{m_2}{m_1 + m_2} = 0.0002857696$. Also equatorial radius of Saturn is 60,268 km., polar radius of Saturn is 54,364 km. and

distance between Sun and Saturn is 1433000000 km. So, according to the equation (1.4.19), oblateness coefficient $A_2 = 6.59158 \times 10^{-11}$. The equatorial plane of the Saturn is coincident with the plane of motion and studied only the planar case. Equations (1.4.12) through (1.4.16) are equations of motion of secondary body. Mean motion n is given by equation (1.4.17) and mass reduction factor q is given by equation (1.4.18). It should be noted that throughout this chapter A_2 is taken as actual oblateness of Saturn and q is taken as variable.

In order to determine the orbital elements of the secondary body at any instant it is necessary to know its position and velocity, which correspond to a point in a four dimensional phase space. For the PSS method, the equations of motion are integrated in (x, y) variables using a Runge–Kutta–Gill fourth order variable or fixed step–size integrator. The initial conditions are selected along the x –axis. By defining a plane, say $y = 0$, in the resulting three dimensional space the values of x and \dot{x} can be plotted every time the particle has $y = 0$, whenever the trajectory intersects the plane in a particular direction, say $\dot{y} > 0$. This section is obtained by fixing a plane in the phase space and plotting the points when the trajectory intersects this plane in a particular direction. We have constructed PSS on the $x - \dot{x}$ plane. The initial values were selected along the Ox –axis by using intervals of length 0.001 and for few cases 0.0001. The magnitude of the velocity vector is determined from its functional dependence on the Jacobi constant. By giving different value of Jacobi constant we can plot the trajectories, and then we can do analysis of orbits. According to Kolmogorov–Arnold–Moser (KAM) theory, if there are smooth and well defined islands, then the trajectory is likely to be regular and the islands correspond to oscillation around a periodic orbit. As the curves shrink down to a point, the point represents a periodic orbit. Any fuzzy distribution of points in the surfaces of section implies that the trajectory is chaotic.

Jacobi constant C is a parameter but its value is not selected arbitrarily. Using equation (1.4.21) we can obtain maximum value of C such that \dot{y}^2 is positive. Let the maximum value of C be denoted by C_M . The value of C is selected from the range $1 \leq C \leq C_M$. This value of C is referred to as admissible value of C . This range of C is depending on the value of parameter q . In other words, we can find admissible value of C such that velocity of secondary body is real for each value of q . The mass reduction factor $q = 0.9$ gives C_M as 2.807. Thus, for $q = 0.9$ admissible range of C is $[1, 2.807]$. For all $x \in [0, 1]$, velocity \dot{y} of secondary body

is real for each pair of $(q, C) = (0.9, C)$, where $C \in [1, 2.807]$. If $C = 2.808$ then for same q , \dot{y}^2 becomes negative for $x \in [0.9290, 0.9510]$. This is the excluded region for secondary body as \dot{y}^2 admits negative values. So, velocity \dot{y} of secondary body becomes complex. This indicates trajectory of secondary body will never pass through the interval $[0.9290, 0.9510]$.

For $q = 1$, admissible range of C is $[1, 3.018]$. Recall that $q = 1$ indicates that there is no perturbation due to solar radiation pressure. Figure 2.1 shows PSS for $C = 3.018$ without perturbation due to solar radiation pressure and periodic orbit lying at the center of the island. This periodic orbit is Saturn centered periodic orbit.

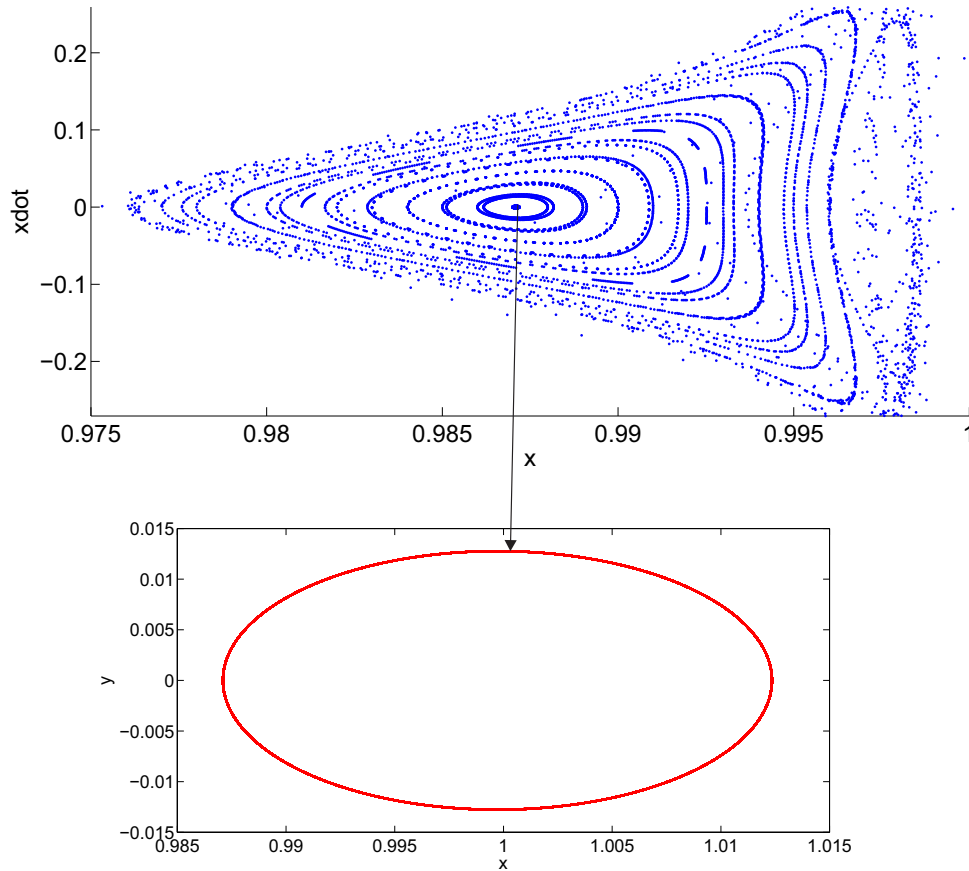


Figure 2.1: PSS of island and periodic orbit at the centre of the island for $q = 1$ and $C = 3.018$.

For $q = 0.9$, we have analyzed the PSS for $1 \leq C \leq 2.8$ with difference in two consecutive values of C , as $\delta C = 0.1$. PSS for $C = 1.0$ contains only two points as shown in Figure 2.2. PSS obtained by taking $q = 0.9$ and $C \in [1.0, 1.7]$, contains

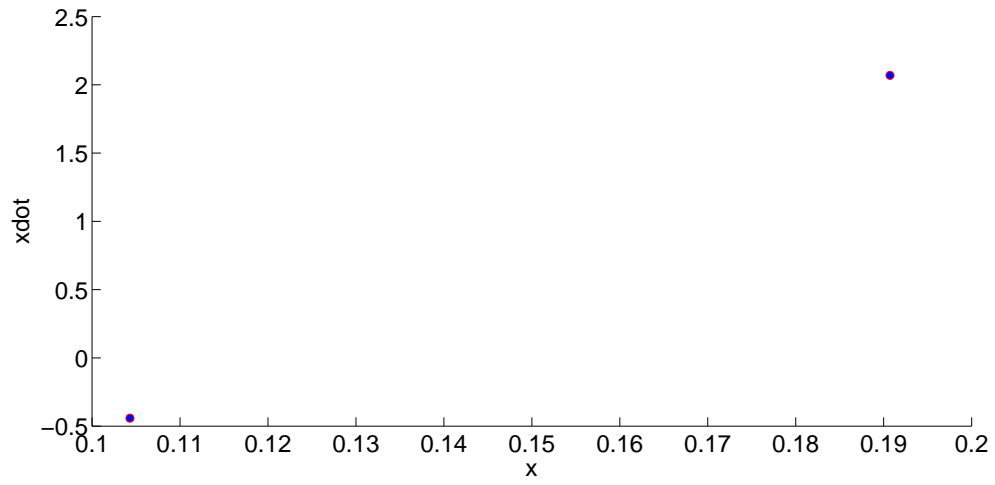


Figure 2.2: PSS for $q = 0.9$ and $C = 1$.

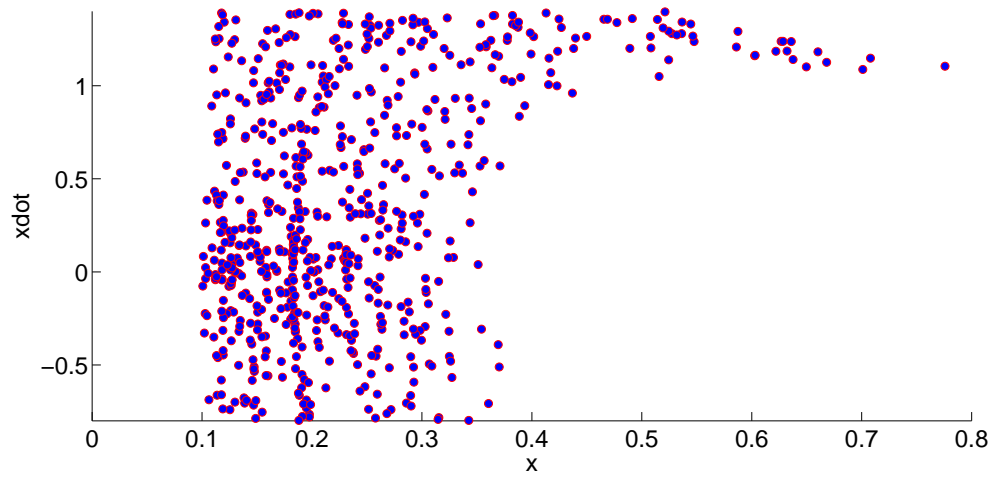


Figure 2.3: PSS for $q = 0.9$ and $C = 1.7$.

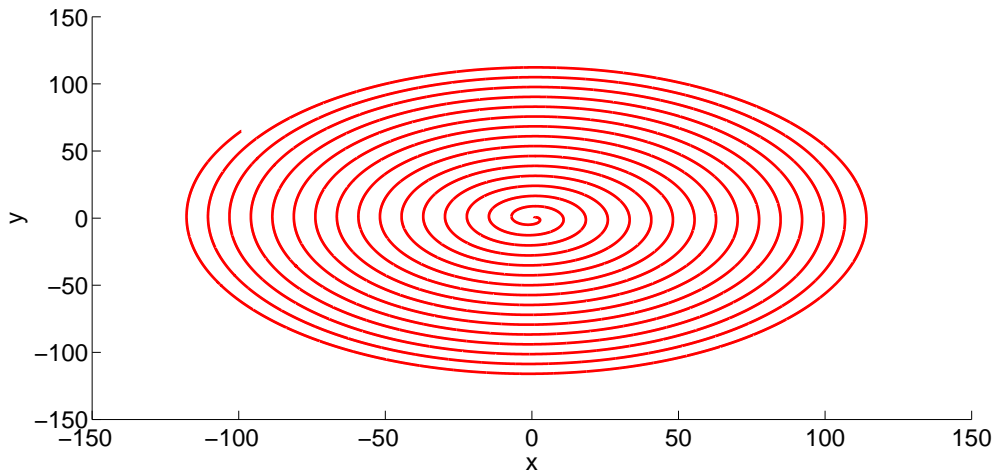


Figure 2.4: Orbit at $x = 0.80320$ for $q = 0.9$ and $C = 1.7$.

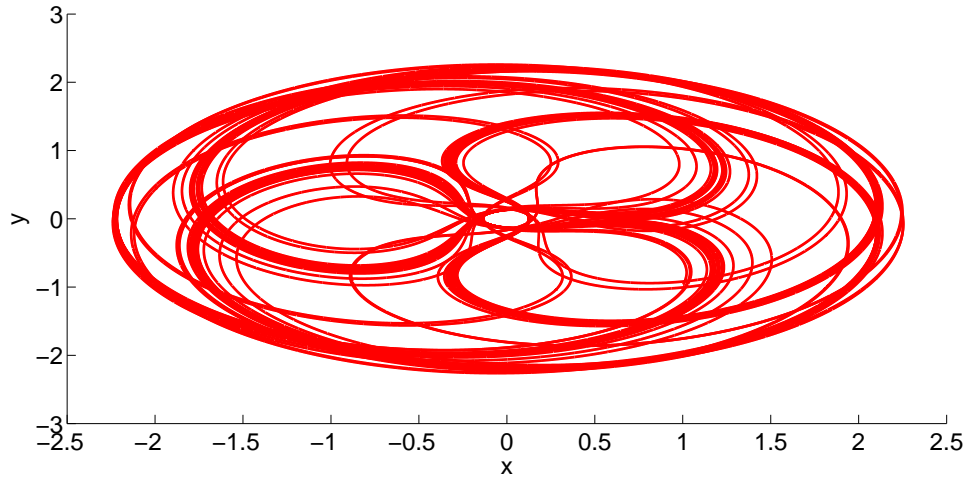


Figure 2.5: Orbit at $x = 0.12690$ for $q = 0.9$ and $C = 1.7$.

only fuzzy distribution of points without any indication of islands. Each and every point of PSS gives only chaotic orbits. PSS for $C = 1.7$ is shown in Figure 2.3. Chaotic orbits at $x = 0.8032$ and $x = 0.1269$ for $(q, C) = (0.9, 1.7)$ are shown in Figures 2.4 and 2.5, respectively.

First quasi-periodic orbit obtained at $x = 0.1168$ for $(q, C) = (0.9, 1.8)$ is located at the center of the island as shown in Figure 2.6. This is the first Sun centered quasi-periodic orbit when $q = 0.9$.

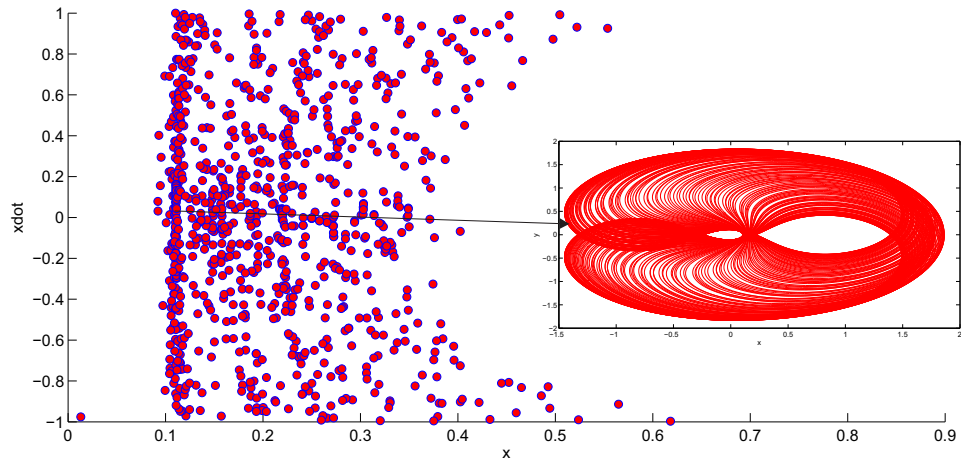


Figure 2.6: PSS and orbit lying on the centre of the island at $x = 0.11680$ for $q = 0.9$ and $C = 1.8$.

By observing PSS for different values of C in the interval $[1.0, 2.8]$, it is concluded that as value of C increases, the number of islands increases and as a result the

number of periodic and quasi-periodic orbits increases.

2.2.1 Sun centered periodic orbits

Here, we mainly concentrate on one of the major islands which gives Sun centred orbit and analyze its nature for different Jacobi constant C . Each PSS is formed between two primaries: the Sun and Saturn located at $(-\mu, 0)$ and $(1 - \mu, 0)$ respectively. Figures 2.7 and 2.8 are divided into three parts. First part of both figures show PSS for $(q, C) = (0.9, 2.79)$ and $(0.9, 2.8)$, respectively. Second part shows enlarged view of the island on which study is focused and third part shows prograde Sun centered periodic orbit corresponding to the center of the island.

Figure 2.9 depicts variation in location of Sun centered periodic orbit with C in the range $[2.785, 2.8]$ for $q = 0.9$. It can be observed that as C increases location of periodic orbit moves towards 1. From analysis of one of the major islands and Sun centered periodic orbit for $q = 0.9$, it is concluded that as C increases location of periodic orbit moves towards Saturn. Semi-major axis a and eccentricity e of the Sun centered periodic orbit are given by equations (1.5.48) through (1.5.51). For Sun centered periodic orbits, Figure 2.10 and Figure 2.11 show that as C increases semi-major axis increases and eccentricity decreases.

By reducing perturbation due to solar radiation pressure up to $q = 0.9845$, the admissible range of C is obtained as $[1, 2.985]$. $C = 2.986$ gives negative \dot{y}^2 within region $x = 0.948$ to $x = 0.960$. Thus, for $(q, C) = (0.9845, 2.986)$ excluded region is $[0.948, 0.960]$. In other words, if equations of motion are integrated within $[0.948, 0.960]$ then velocity \dot{y} of secondary body becomes complex.

For $(q, C) = (0.9, 2.808)$ excluded region is $[0.9290, 0.9510]$ and for $(q, C) = (0.9845, 2.986)$ it is $[0.948, 0.960]$. Thus, perturbation due to solar radiation pressure affects the admissible range of Jacobi constant. Also, it is observed that excluded region is shifted towards Saturn as q moves towards 1.

Figures 2.12 and 2.13 are also divided into three parts. First part of Figures 2.12 and 2.13 show PSS for $q = 0.9845$ with $C = 2.985$ and 2.975 respectively. Second part shows magnified form of the island on which study is focused and third part show Sun centered periodic orbit lying at centre of the island.

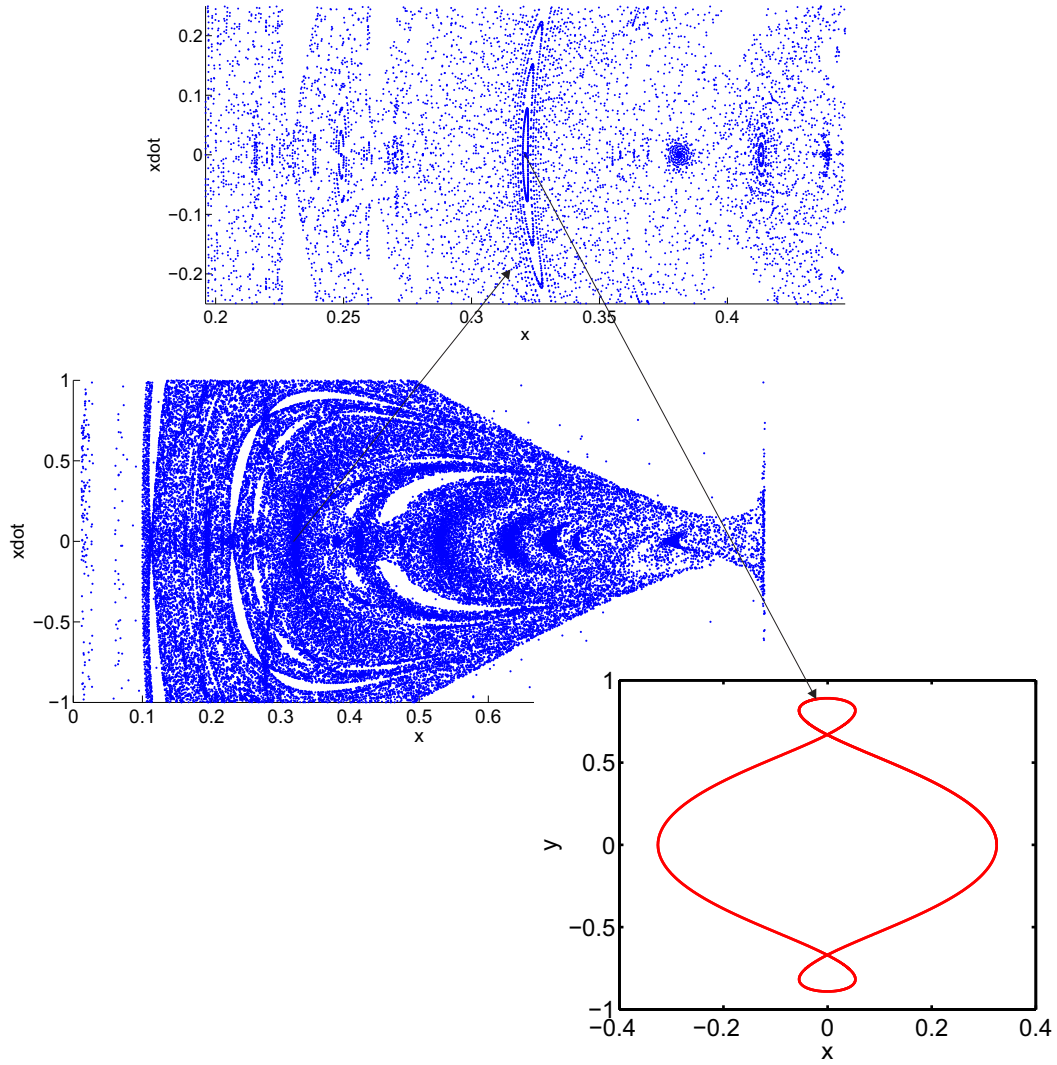


Figure 2.7: PSS, magnified form of one of the islands near $x = 0.32$ and periodic orbit lying at $x = 0.32490$ for $q = 0.9$ and $C = 2.79$.

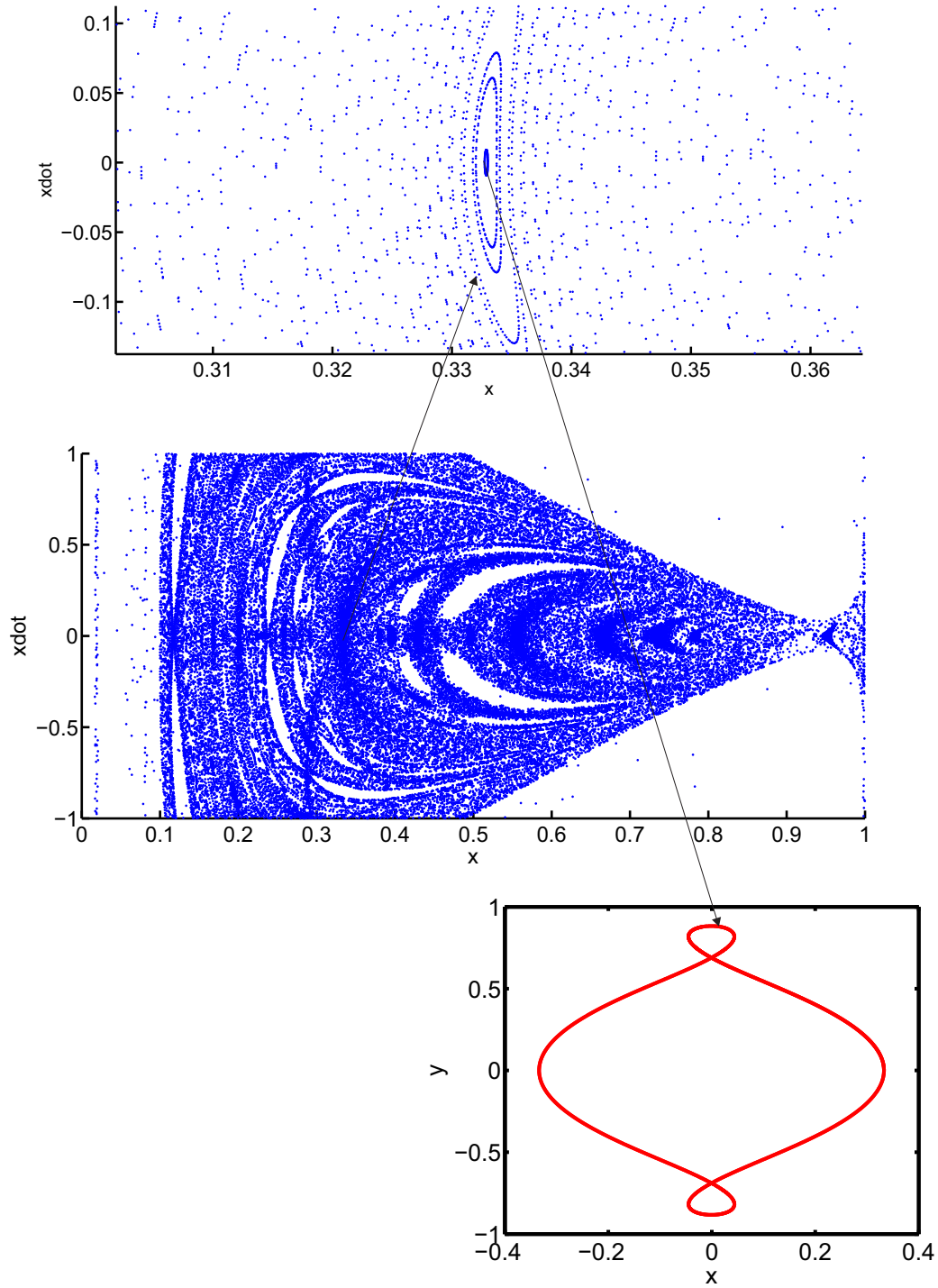


Figure 2.8: PSS, magnified form of one of the islands near $x = 0.33$ and periodic orbit lying at $x = 0.33286$ for $q = 0.9$ and $C = 2.8$.

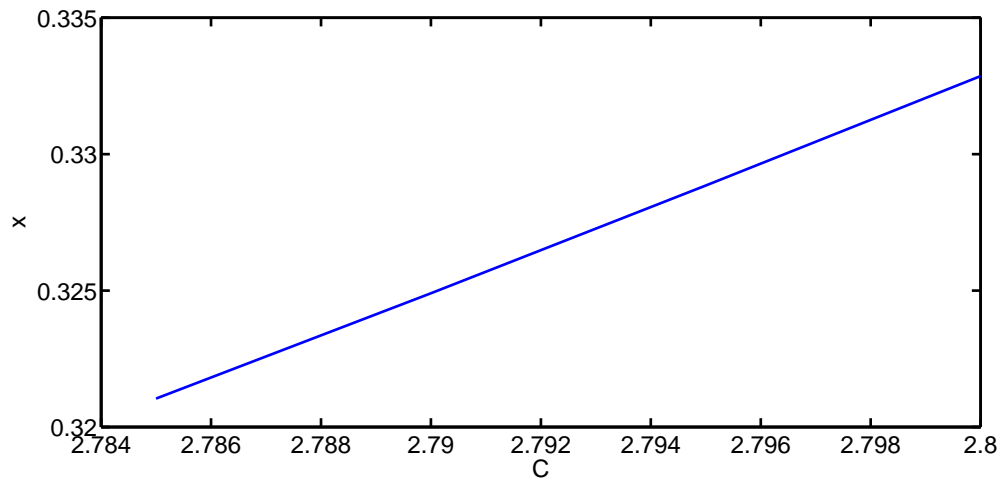


Figure 2.9: Location of Sun centered periodic orbit Vs Jacobi constant C for $q = 0.9$.

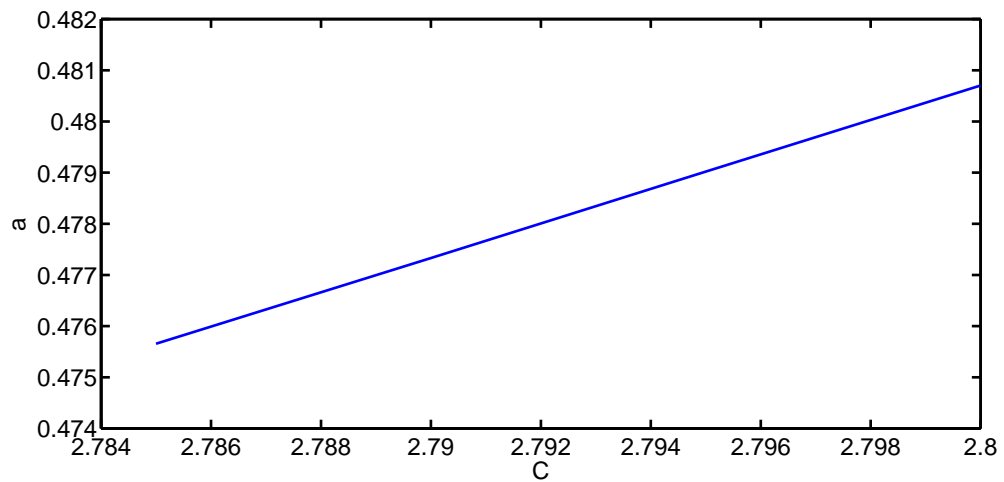


Figure 2.10: Semi-major axis of Sun centered periodic orbit Vs Jacobi constant C for $q = 0.9$.

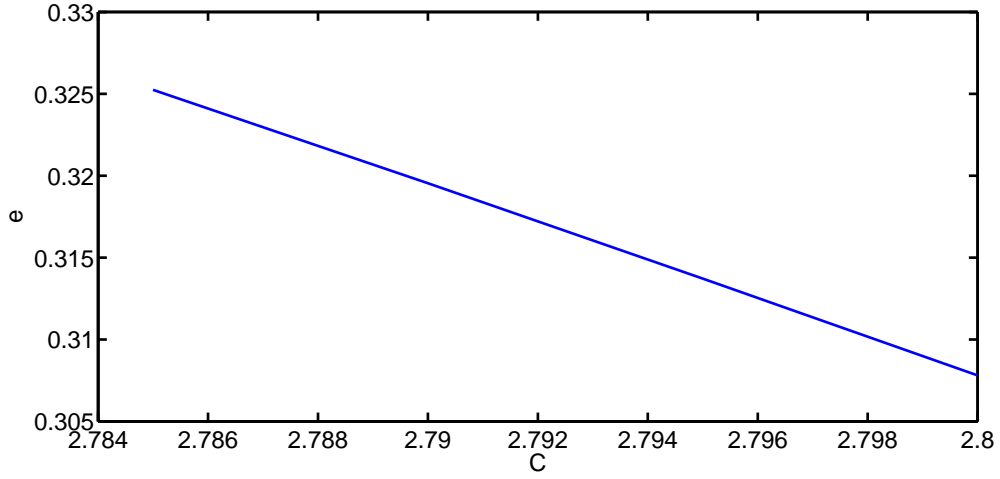


Figure 2.11: Eccentricity of Sun centered periodic orbit Vs Jacobi constant C for $q = 0.9$.

For $q = 1$ admissible range of C is $[1, 3.018]$. $(q, C) = (1, 3.019)$ gives excluded region $[0.946, 0.964]$. In Figures 2.14 and 2.15, first part show PSS for $q = 1$ with $C = 2.985$ and 2.975 , respectively. Second part show the magnified form of the island and the third part show Sun entered periodic orbit lying at the center of the island. From the analysis of island and its corresponding periodic orbits it is concluded that increment in Jacobi constant is responsible for shifting of location of periodic orbits towards Saturn when $q = 1$ and $q = 0.9845$ as shown in Figure 2.16. For Sun centered periodic orbits, Figures 2.17 and 2.18 show that as C increases semi-major axis of periodic orbit increases and eccentricity of periodic orbit decreases.

For obtaining the effect of solar radiation pressure on Sun centered periodic orbit we have taken same range of C for $q = 1$ and $q = 0.9845$. In other words, we have studied PSS corresponding to $(q, C) = (1, C)$ and $(0.9845, C)$, where $C \in [2.97, 2.985]$. For $q = 1$, the shifting of periodic orbits towards Saturn by increasing value of C is shown in Figure 2.16. Third part of figures 2.12 and 2.14 show Sun centered periodic orbit for $C = 2.985$ with $q = 0.9845$ and $q = 1$ respectively. Third part of figures 2.14 and 2.15 show Sun centered periodic orbit for $C = 2.985$ and 2.975 with $q = 1$.

Figure 2.16 shows effect of solar radiation pressure on Sun centered periodic orbit obtained for a given C . It is concluded that solar radiation pressure is responsible for shifting of the location of periodic orbits towards Saturn which is shown in Figure 2.17. It is observed from Figure 2.17 that as C increases semi-major axis increases.

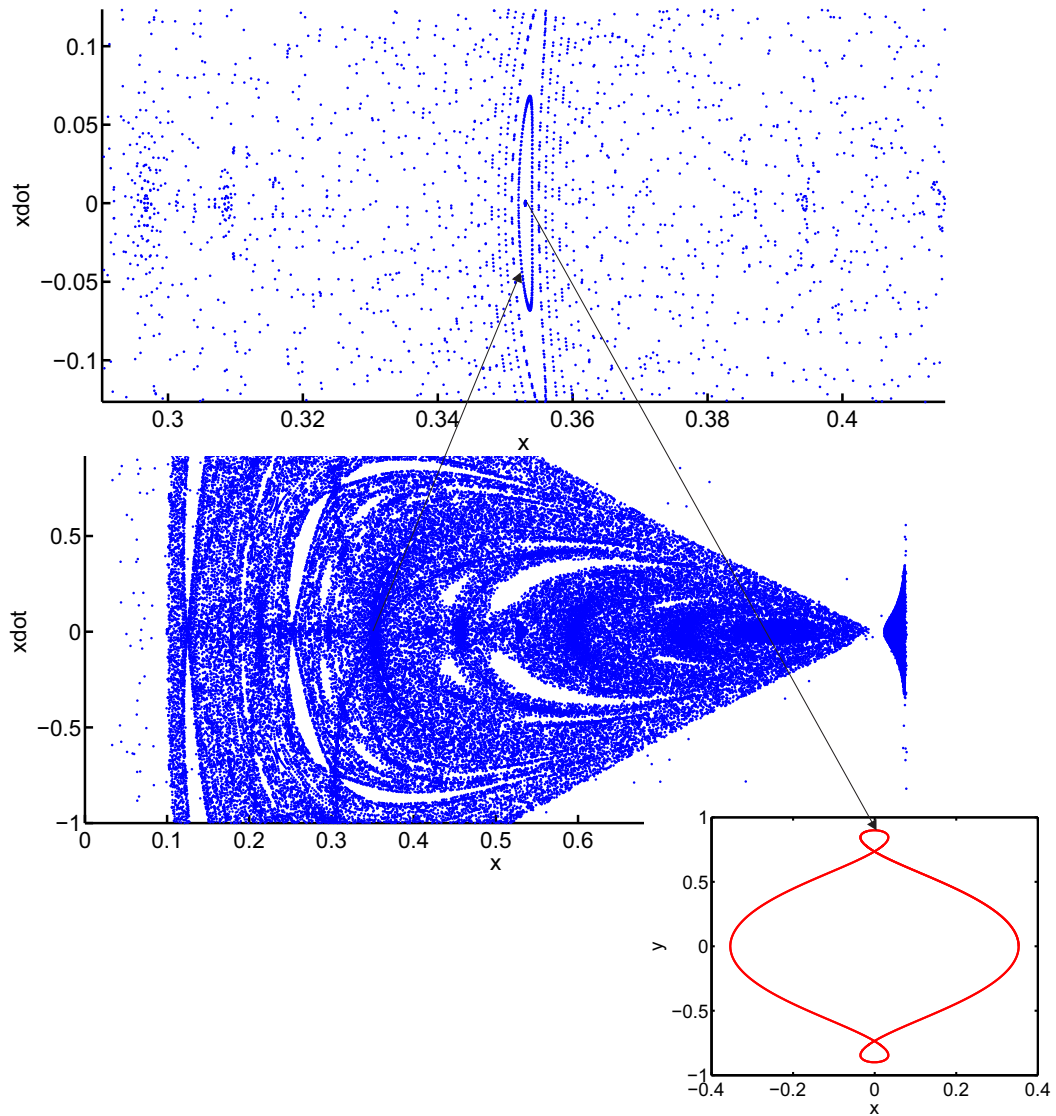


Figure 2.12: PSS, magnified form of one of the islands near $x = 0.35$ and periodic orbit lying at $x = 0.352983$ for $C = 2.985$ and $q = 0.9845$.

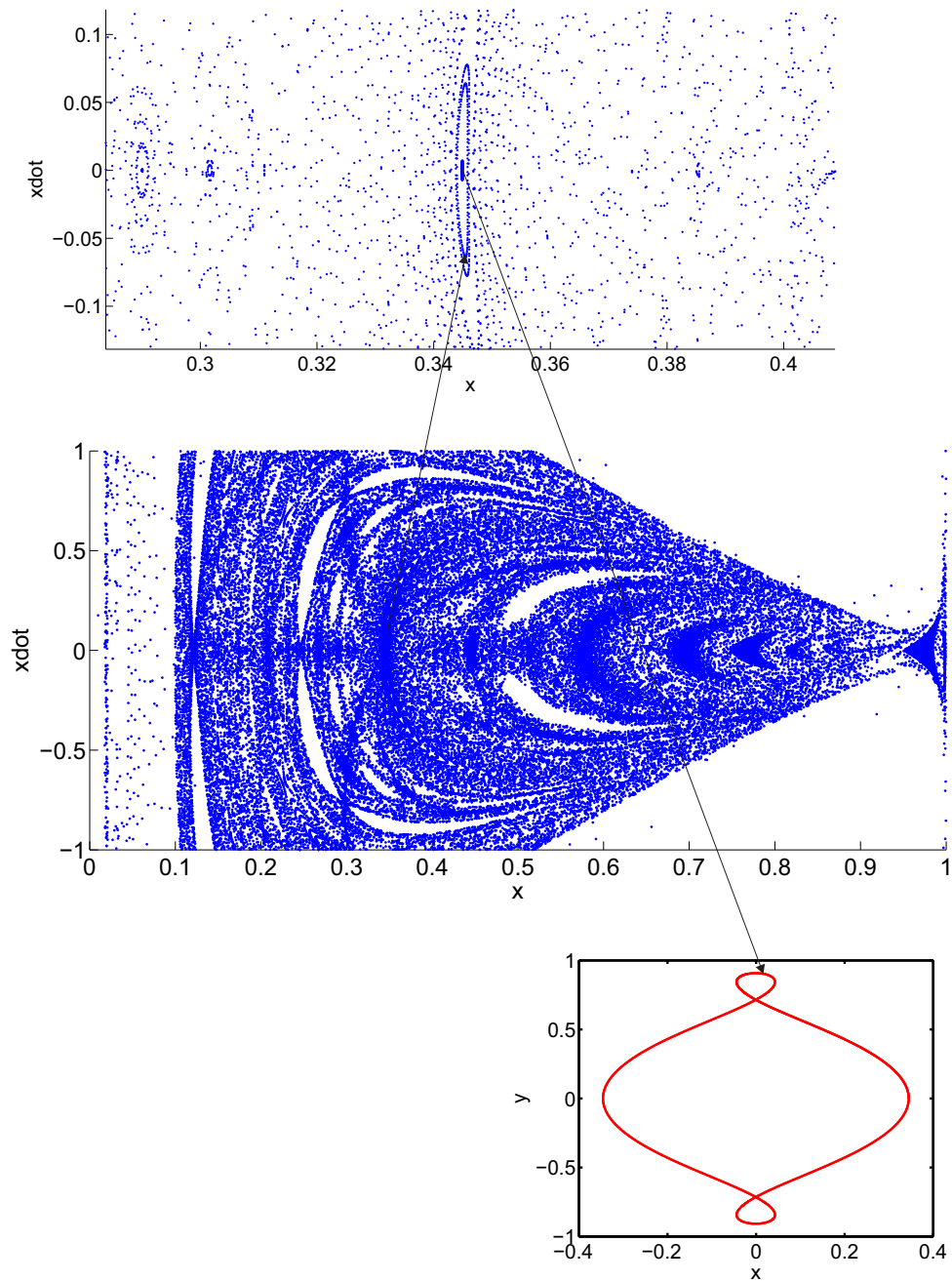


Figure 2.13: PSS, magnified form of one of the islands near $x = 0.34$ and periodic orbit lying at $x = 0.34490$ for $C = 2.975$ and $q = 0.9845$.

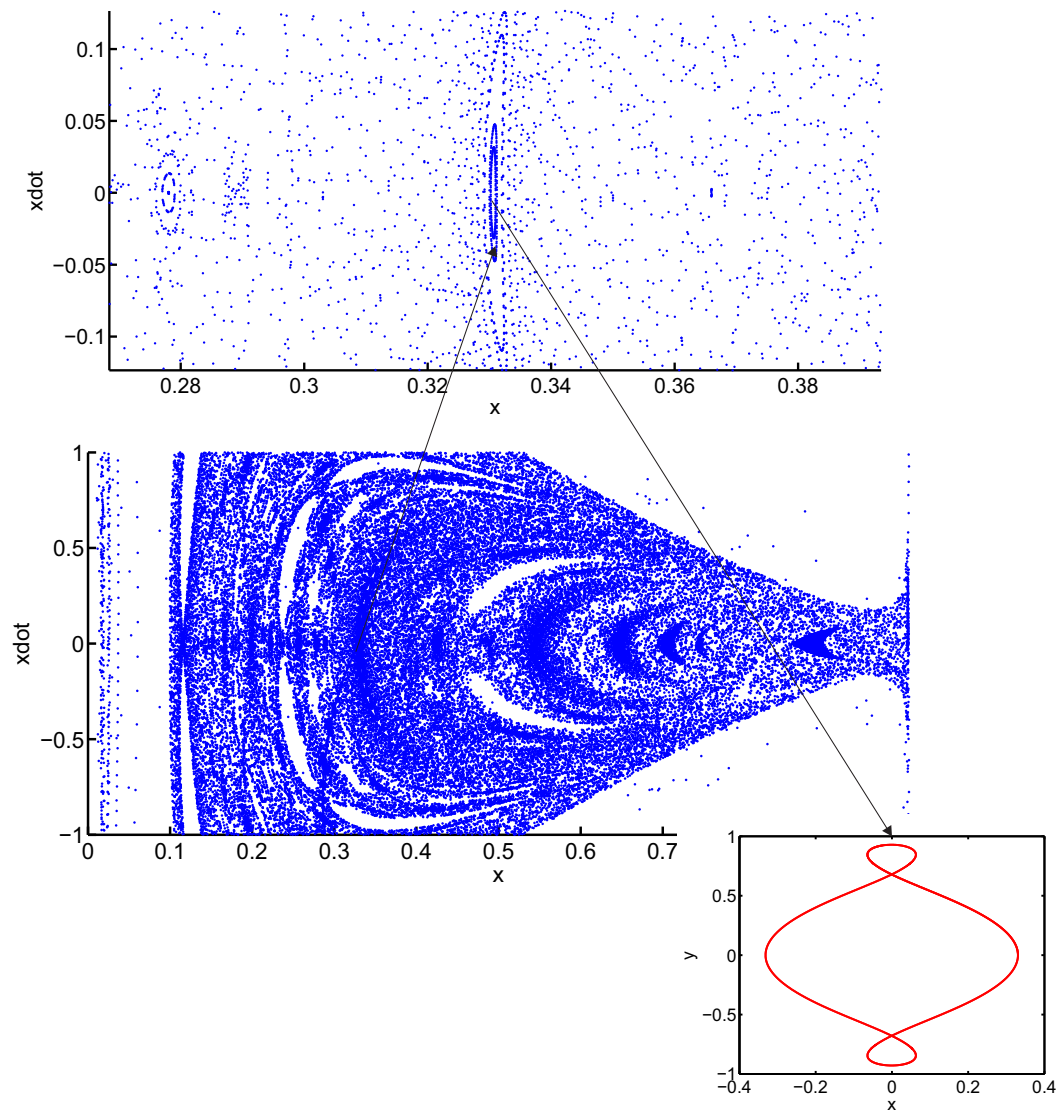


Figure 2.14: PSS, magnified form of one of the islands near $x = 0.33$ and periodic orbit lying at $x = 0.33060$ for $C = 2.985$ and $q = 1$.

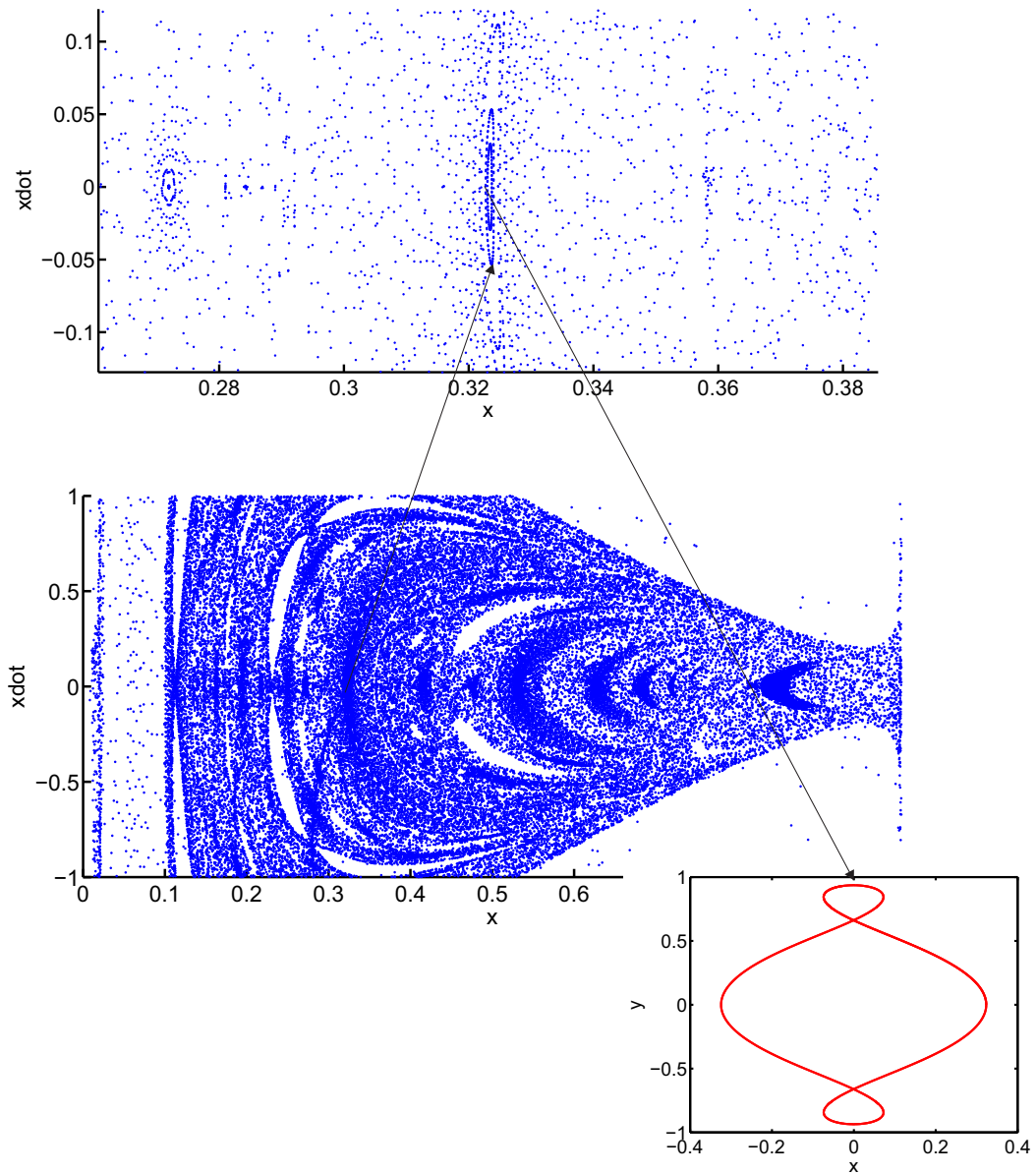


Figure 2.15: PSS, magnified form of one of the islands near $x = 0.32$ and periodic orbit lying at $x = 0.32335$ for $C = 2.975$ and $q = 1$.

It can be noticed that as perturbation due to solar radiation pressure decreases, semi-major axis of periodic orbits for a given value of C increases. Figure 2.18 shows that as C increases, eccentricity of the periodic orbit decreases. It is concluded that solar radiation pressure affects eccentricity of Sun centered periodic orbit for given C .

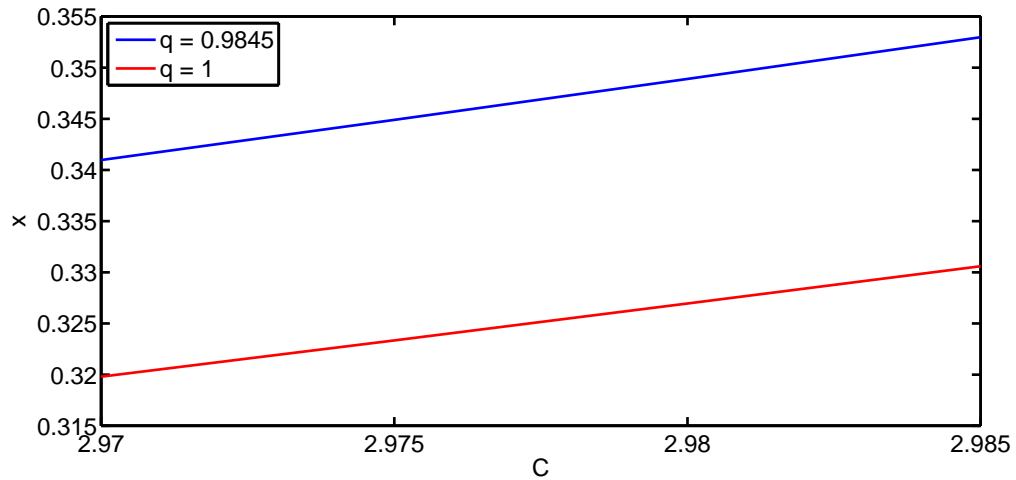


Figure 2.16: Variation in location of Sun centered periodic orbit for $q = 0.9845$ and $q = 1$.

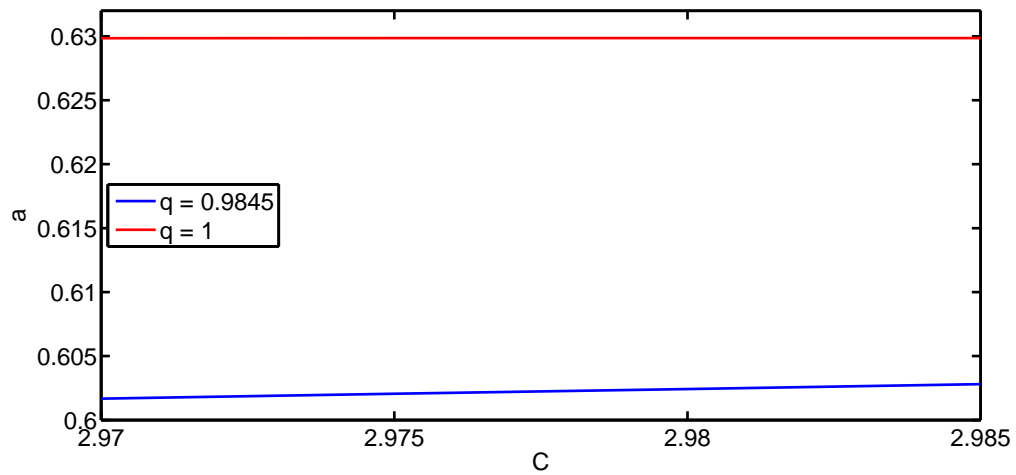


Figure 2.17: Variation in semi-major axis of Sun centered periodic orbit for $q = 0.9845$ and $q = 1$.

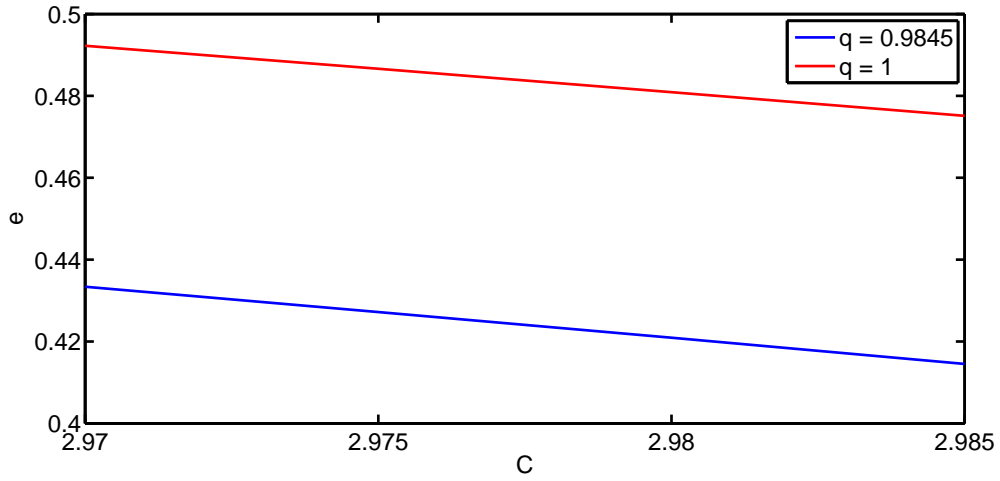


Figure 2.18: Variation in eccentricity of Sun centered periodic orbit for $q = 0.9845$ and $q = 1$.

2.2.2 Saturn centered periodic orbits

By considering $q = 0.9345$, admissible range of C is $[1, 2.88]$. $C = 2.881$ gives negative \dot{y}^2 in the region $0.937 \leq C \leq 0.956$, which is excluded region for secondary body as velocity becomes complex. Also, for $q = 0.9645$ admissible range of C is $[1, 2.943]$. $C = 2.944$ gives $[0.945, 0.957]$ as excluded region. It is observed that excluded region becomes smaller as q increases and the excluded region slightly shifted towards Saturn.

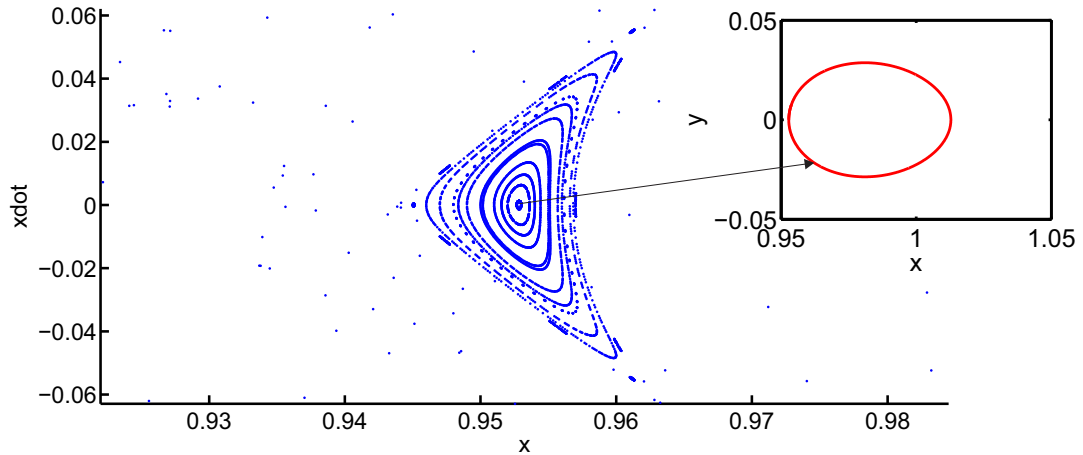


Figure 2.19: PSS of island for $C = 2.80$ and $q = 0.9$.

PSS of island corresponding to Saturn centered periodic orbit for $C = 2.8$ with $q = 0.9, 0.9345, 0.9645$ and 1 are shown in Figures 2.19, 2.20, 2.21 and 2.22, respectively.

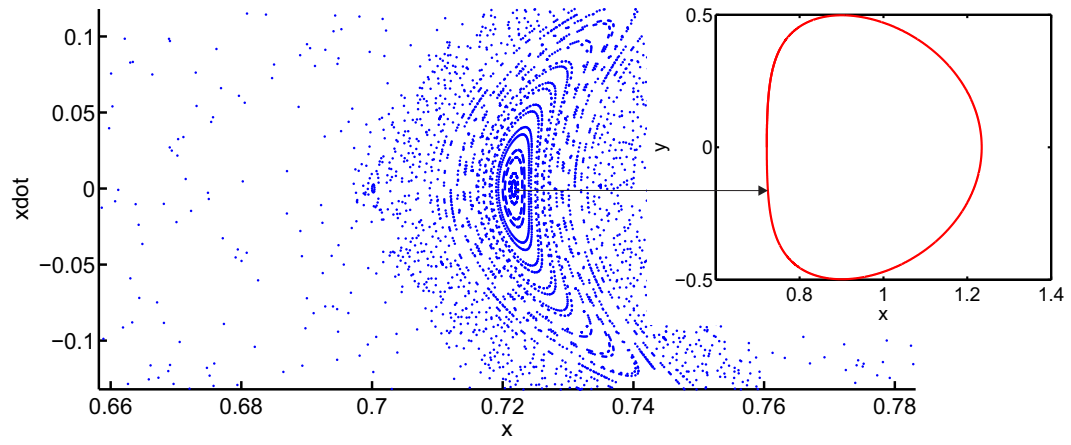


Figure 2.20: PSS of island for $C = 2.80$ and $q = 0.9345$.

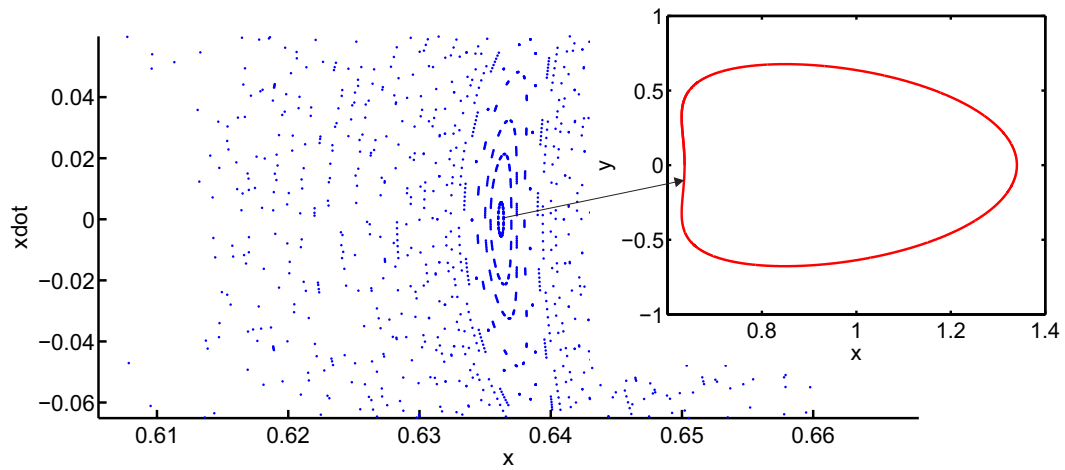


Figure 2.21: PSS of island for $C = 2.80$ and $q = 0.9645$.

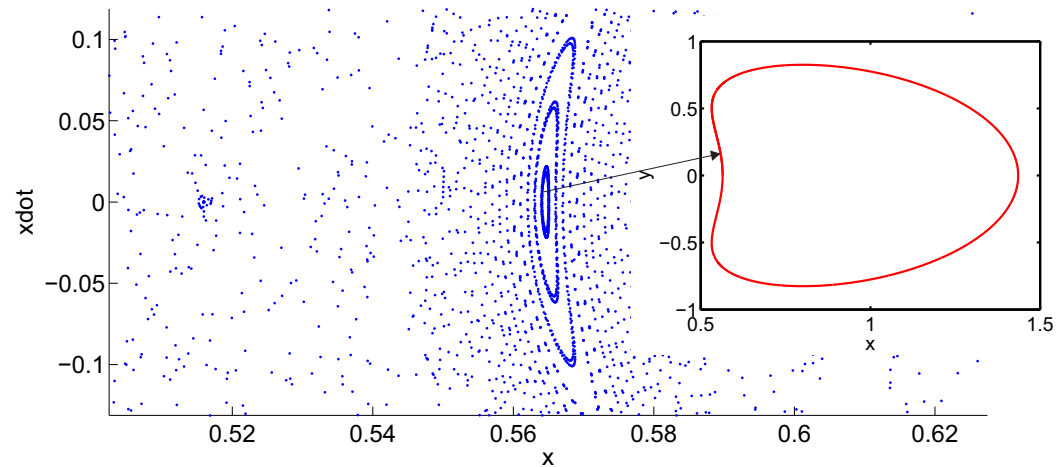


Figure 2.22: PSS of island for $C = 2.80$ and $q = 1$.

Center of the island gives Saturn centered periodic orbit at $x = 0.95285, 0.72165, 0.6365$ and at 0.56455 , respectively.

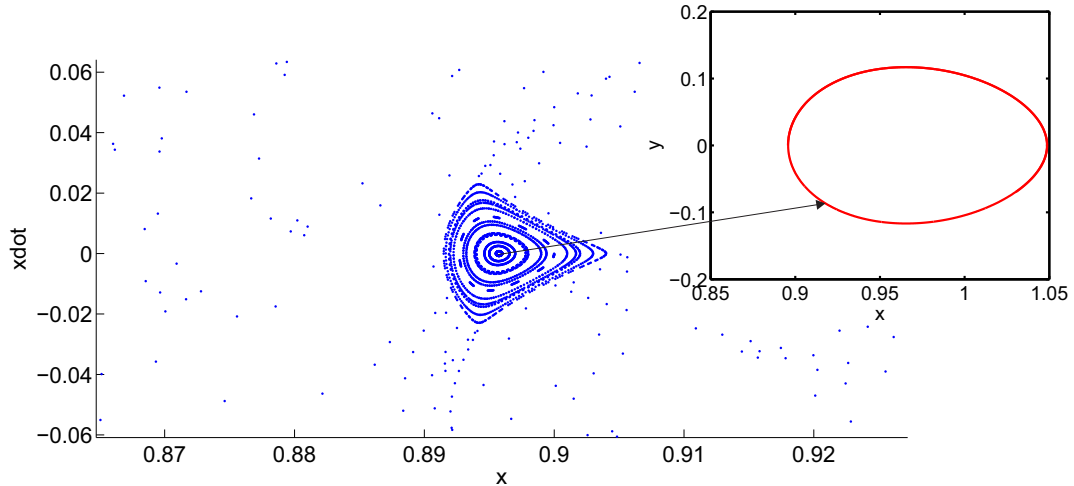


Figure 2.23: PSS of island for $C = 2.79$ and $q = 0.9$.

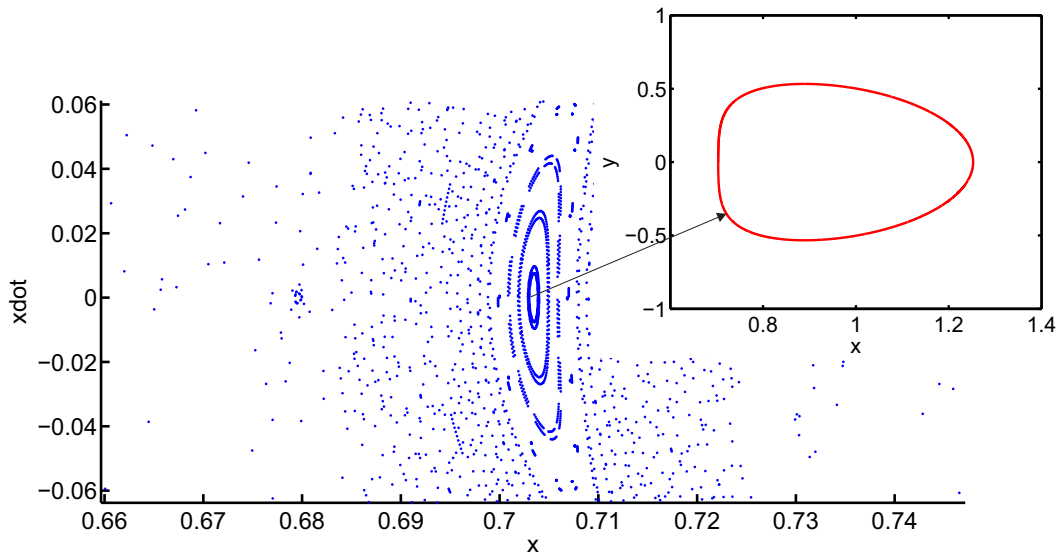


Figure 2.24: PSS of island for $C = 2.79$ and $q = 0.9345$.

Figures 2.23–2.26 show PSS for island corresponding to Saturn centered periodic orbit for $C = 2.79$ with $q = 0.9, 0.9345, 0.9645$ and 1 , respectively. Center of the island gives Saturn centered periodic orbit at $x = 0.8957, 0.70345, 0.62315$ and 0.55435 , respectively.

Figures 2.27–2.30 depict PSS of island for $C = 2.78$ with $q = 0.9, 0.9345, 0.9645$ and 1 , respectively. Center of the island gives Saturn centered periodic orbit at $x = 0.8429, 0.68645, 0.61065$, and 0.54444 , respectively.

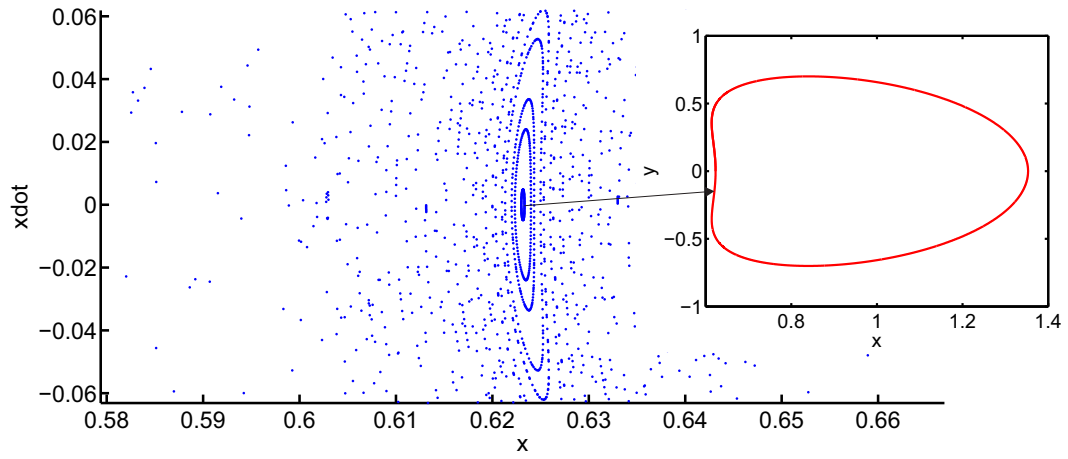


Figure 2.25: PSS of island for $C = 2.79$ and $q = 0.9645$.

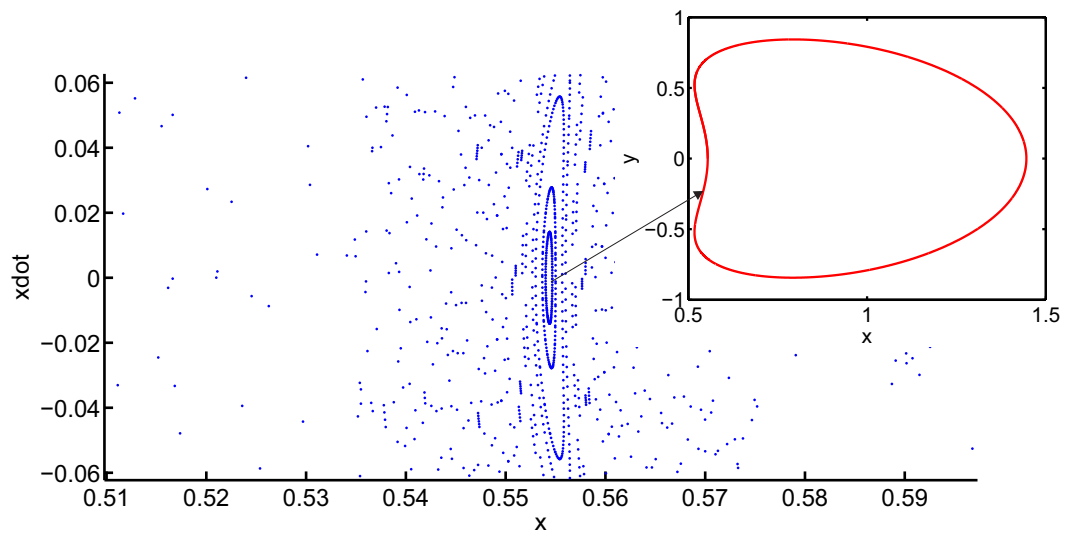


Figure 2.26: PSS of island for $C = 2.79$ and $q = 1$.

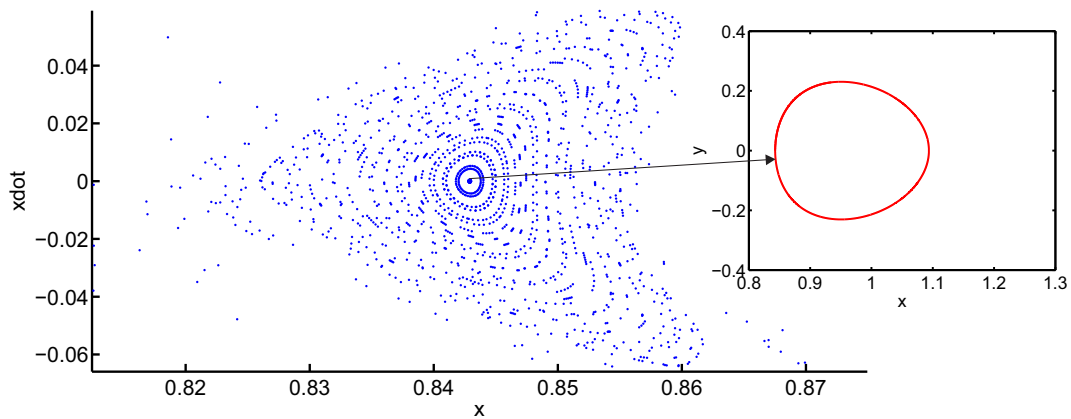


Figure 2.27: PSS of island for $C = 2.78$ and $q = 0.9$.

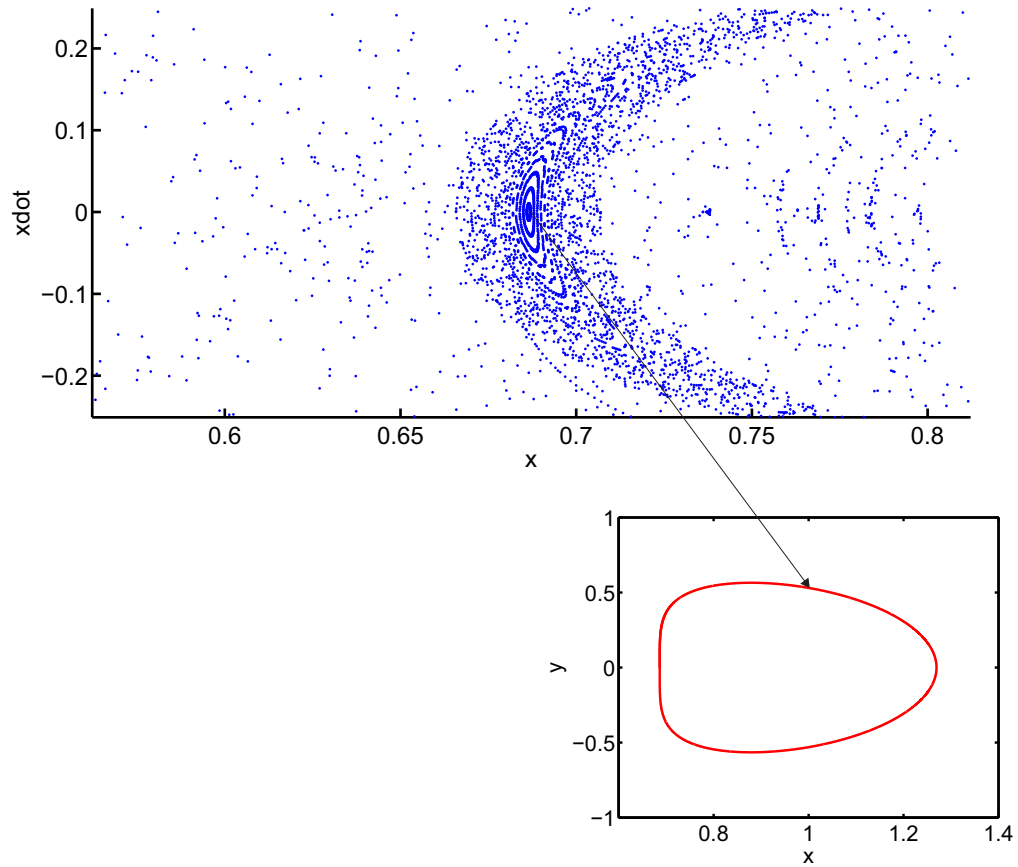


Figure 2.28: PSS of island for $C = 2.78$ and $q = 0.9345$.

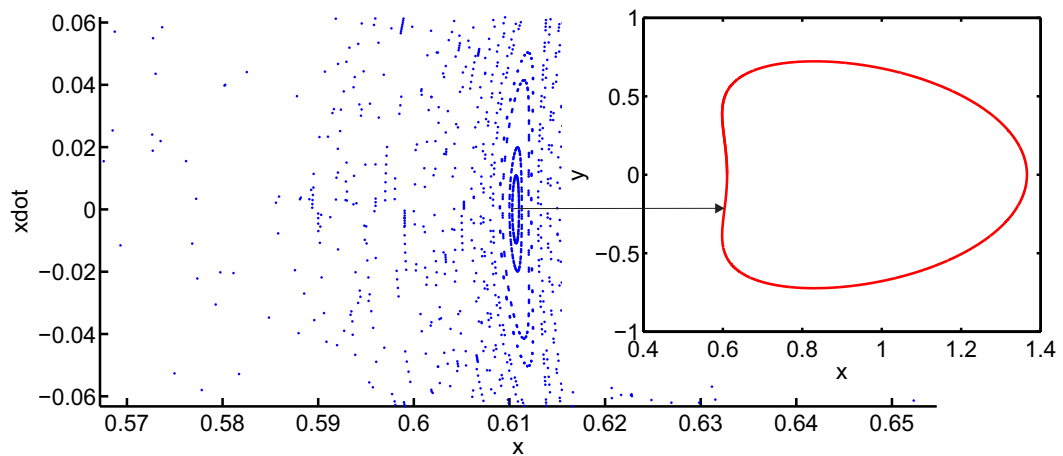


Figure 2.29: PSS of island for $C = 2.78$ and $q = 0.9645$.

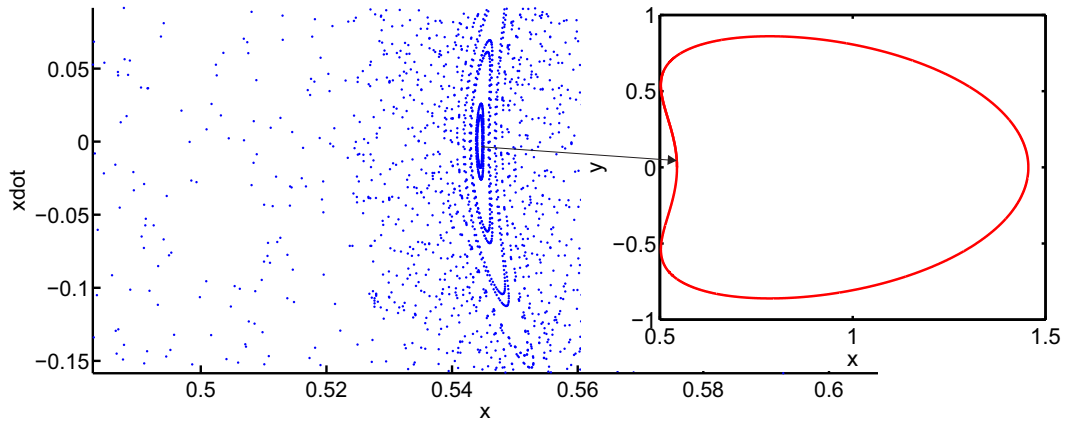


Figure 2.30: PSS of island for $C = 2.78$ and $q = 1$.

From these figures it is observed that for a given value of C , by decreasing perturbation due to solar radiation pressure, Saturn centered periodic orbit moves towards Sun. This is the effect of solar radiation pressure on retrograde Saturn centered periodic orbits. From Figures 2.19, 2.23 and 2.27, it can be observed that for $q = 0.9$, by decreasing C , Saturn centered periodic orbit moves towards Sun. Similar results can be observed in Figures 2.20, 2.24 and 2.28 for $q = 0.9345$, in Figures 2.21, 2.25 and 2.29 for $q = 0.9645$ and in Figures 2.22, 2.26 and 2.30 for $q = 1$.

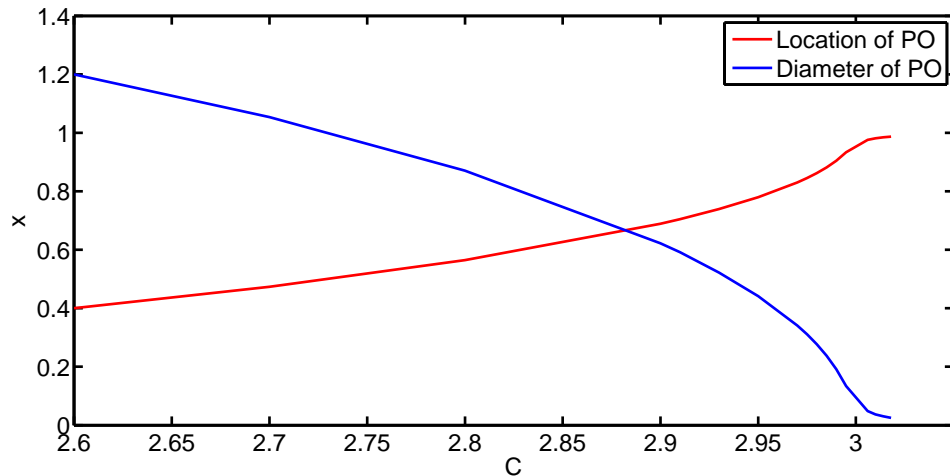


Figure 2.31: Variation in location and diameter of Saturn centered periodic orbit for $q = 1$.

This is the effect of Jacobi constant on Saturn centered retrograde periodic orbits. The shifting of Saturn centered retrograde periodic orbits towards Saturn against C is plotted in Figures 2.31–2.35 for $q = 1, 0.9845, 0.9645, 0.9345$ and 0.9 , respectively. It can be seen that, as the value of C increases the diameter decreases. It should be

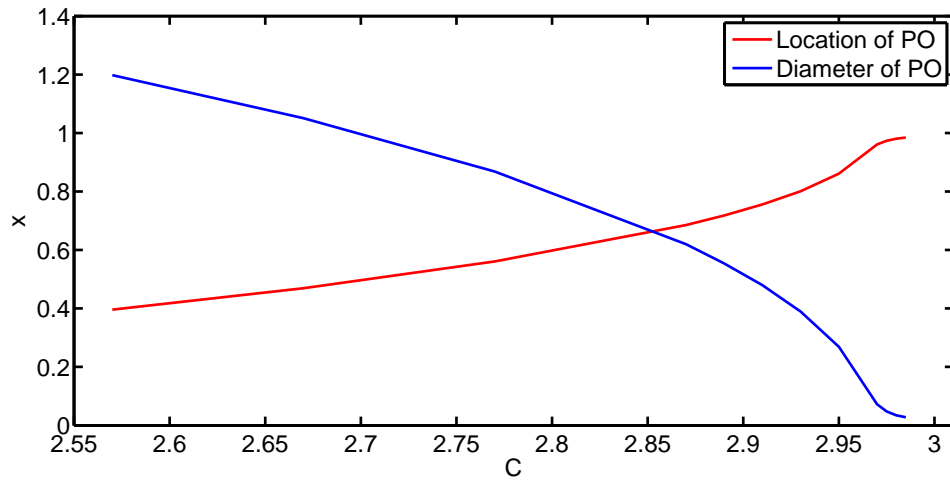


Figure 2.32: Variation in location and diameter of Saturn centered periodic orbit for $q = 0.9845$.

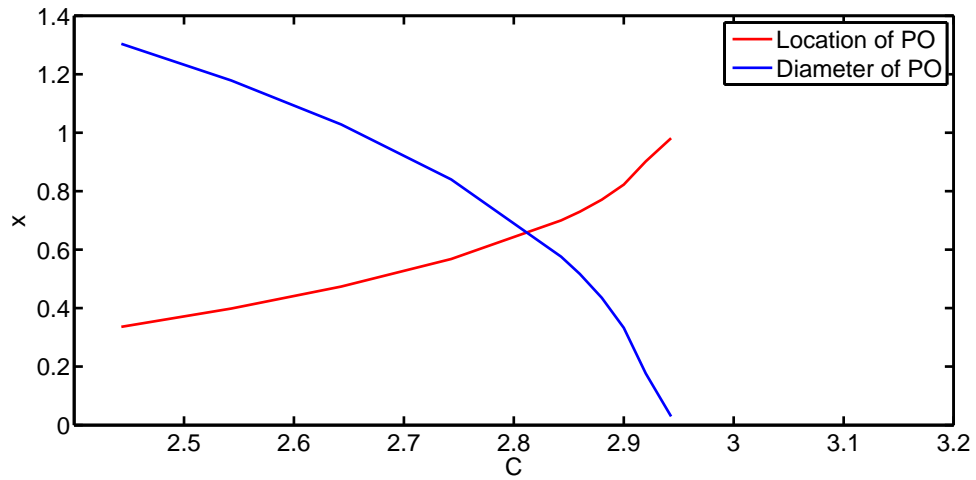


Figure 2.33: Variation in location and diameter of Saturn centered periodic orbit for $q = 0.9645$.

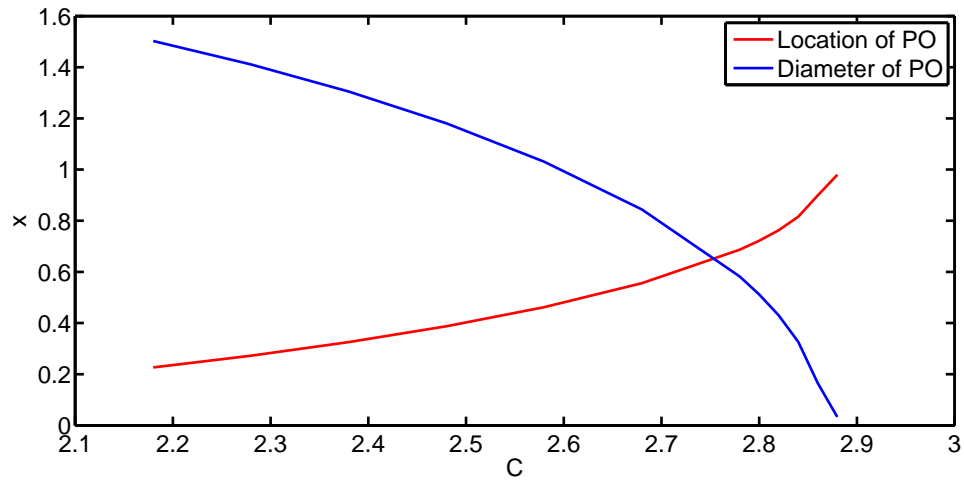


Figure 2.34: Variation in location and diameter of Saturn centered periodic orbit for $q = 0.9345$.

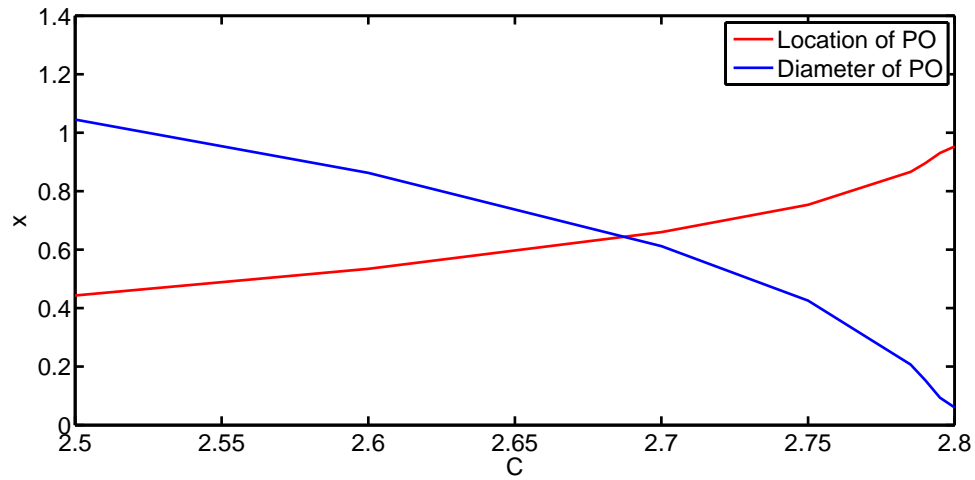


Figure 2.35: Variation in location and diameter of Saturn centered periodic orbit for $q = 0.9$.

noted that for plotting graphs in Figures 2.31–2.36 the same scale is used.

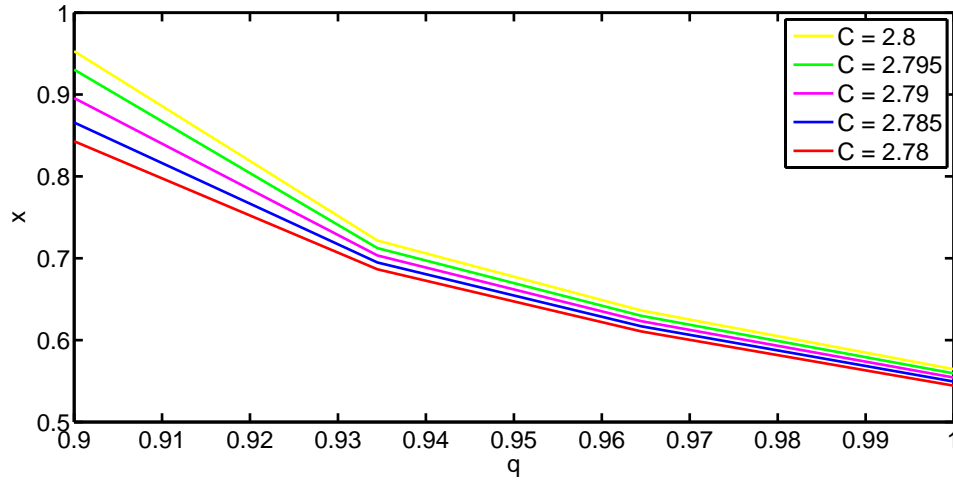


Figure 2.36: Variation in location of periodic orbit for variation in q .

Figure 2.36 shows the variation of location of Saturn centered periodic orbit with variation in perturbation due to q for $C = 2.8, 2.795, 2.79, 2.785$ and 2.78 . It is clear from Figure 2.36 that, for a given C , by reducing perturbation due to solar radiation pressure location of periodic orbit moves towards Sun which is similar to Sun centered periodic orbits.

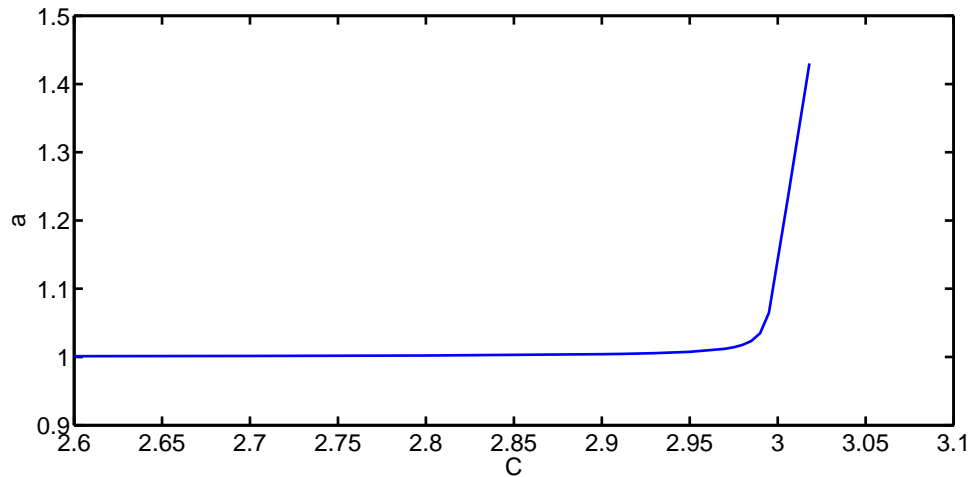


Figure 2.37: Variation in semi-major axis of Saturn centered periodic orbit for $q = 1$.

Figure 2.37 depicts the variation of semi-major axis without perturbation due to solar radiation pressure. It is clear from the graph that as C increases semi-major

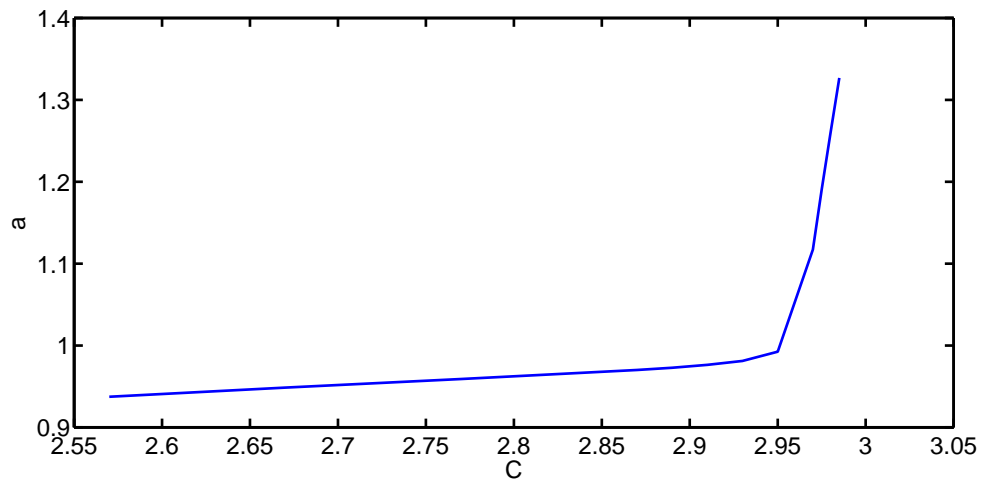


Figure 2.38: Variation in semi-major axis of Saturn centered periodic orbit for $q = 0.9845$.

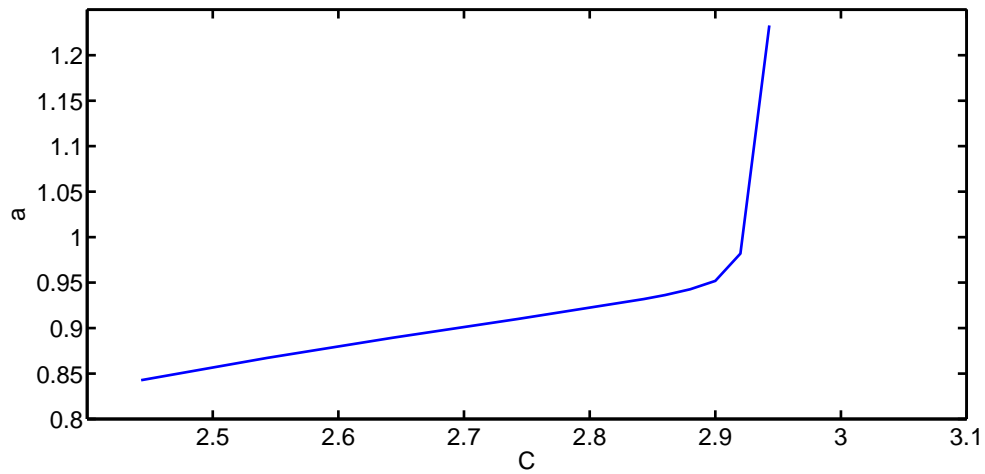


Figure 2.39: Variation in semi-major axis of Saturn centered periodic orbit for $q = 0.9645$.

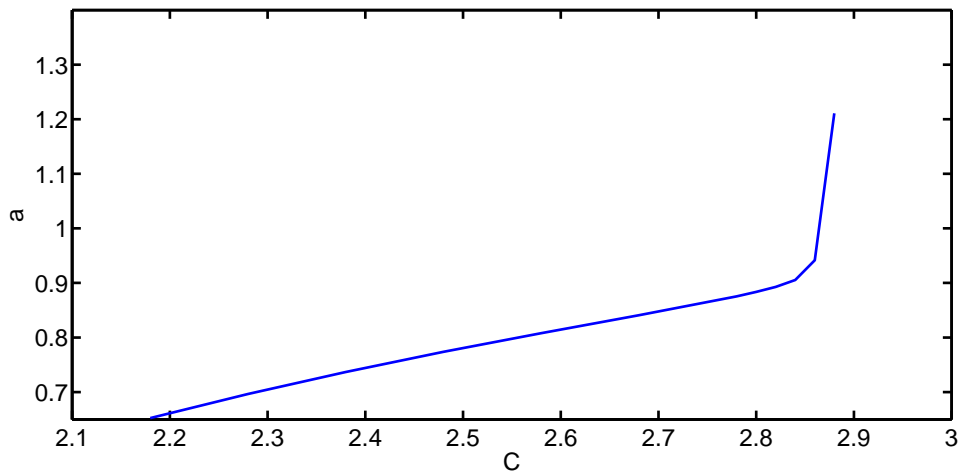


Figure 2.40: Variation in semi-major axis of Saturn centered periodic orbit for $q = 0.9345$.

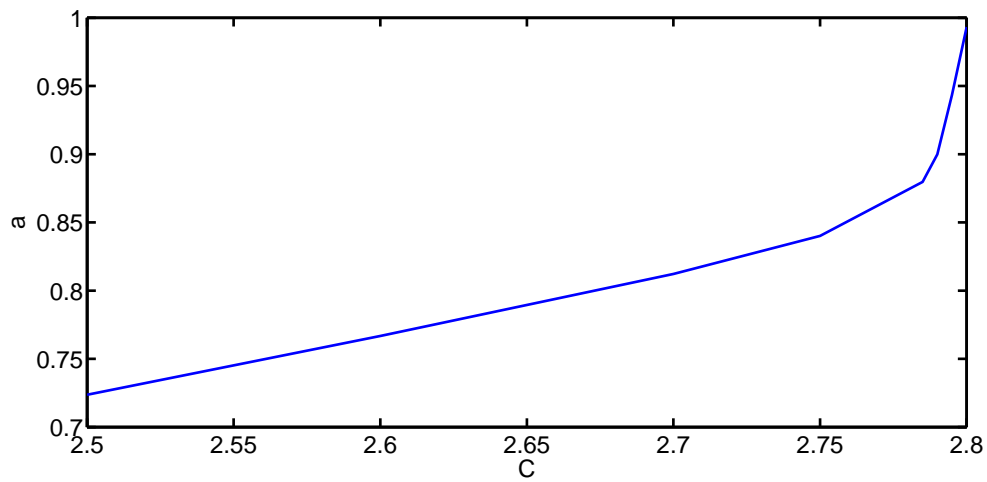


Figure 2.41: Variation in semi-major axis of Saturn centered periodic orbit for $q = 0.9$.

axis increases. Between $C = 2.985$ and $C = 3.018$ the curve takes a steep ascent. For $C = 2.985$ semi-major axis of periodic orbit has value 1.0234 and for $C = 3.018$ it is 1.43022. Figure 2.38 shows variation of semi-major axis for $q = 0.9845$. Observable change in semi-major axis is seen between $C = 2.87$ and $C = 2.97$. For $C = 2.87$ semi-major axis of Saturn centered periodic orbit is 0.97012 and for $C = 2.97$ it is 1.1171. Again a steep ascent of the curve is observed in the graph of semi-major axis against C between $C = 2.97$ and $C = 2.985$. Semi-major axis for $C = 2.985$ is 1.3269.

Figure 2.39 shows variation of semi-major axis for $q = 0.9645$. Steep ascent of the curve in the semi-major axis between $C = 2.9$ and $C = 2.943$. For $C = 2.9$ semi-major axis for Saturn centered periodic orbit is 0.9519 whereas for $C = 2.943$ it is 1.2328. Figure 2.40 depicts the variation of semi-major axis for $q = 0.9345$. Observable change can be observed between $C = 2.78$ and $C = 2.88$. For $C = 2.78$ semi-major axis of Saturn centered periodic orbit is 0.8754 and for $C = 2.88$ it is 1.2109.

Figure 2.41 shows uniform change in semi-major axis of Saturn centered periodic orbits for $q = 0.9$.

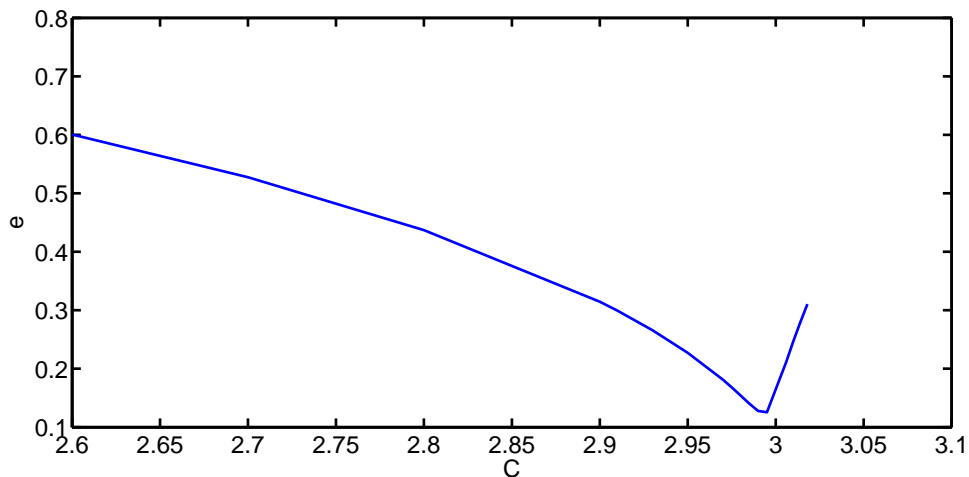


Figure 2.42: Variation in eccentricity of Saturn centered periodic orbit for $q = 1$.

Figure 2.42 shows the variation of eccentricity of Saturn centered periodic orbit for $q = 1$ that is without perturbation due to solar radiation pressure. It is clear from the graph as C increases eccentricity decreases. But the steep ascent of the curve is seen between $C = 2.985$ and $C = 3.018$. For $C = 2.985$ eccentricity is 0.14036 and

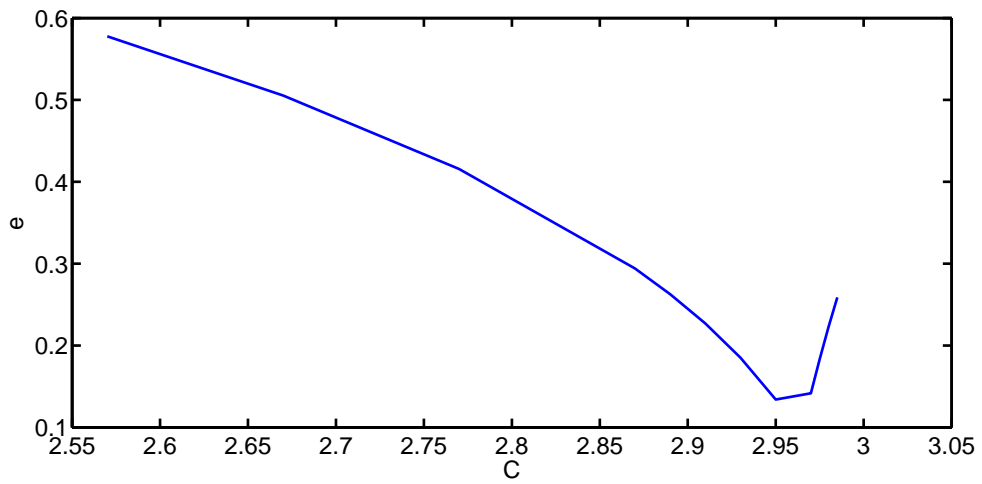


Figure 2.43: Variation in eccentricity of Saturn centered periodic orbit for $q = 0.9845$.

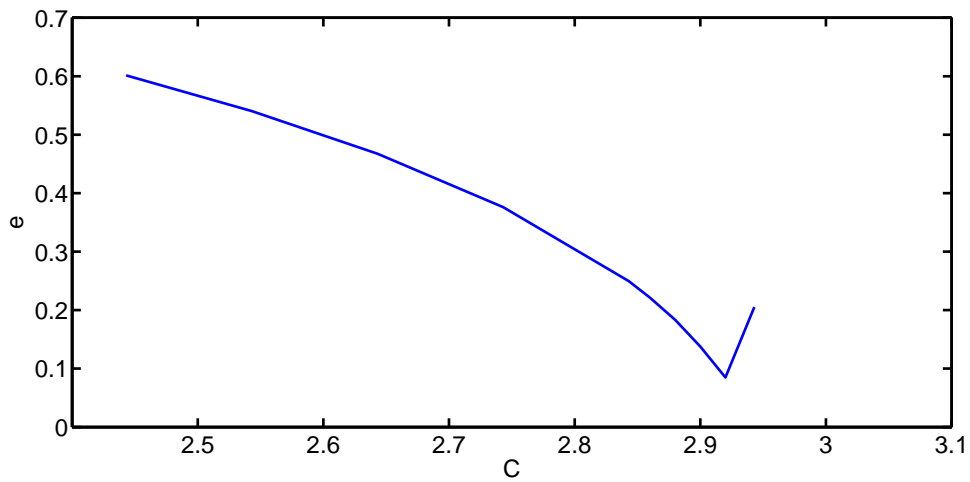


Figure 2.44: Variation in eccentricity of Saturn centered periodic orbit for $q = 0.9645$.

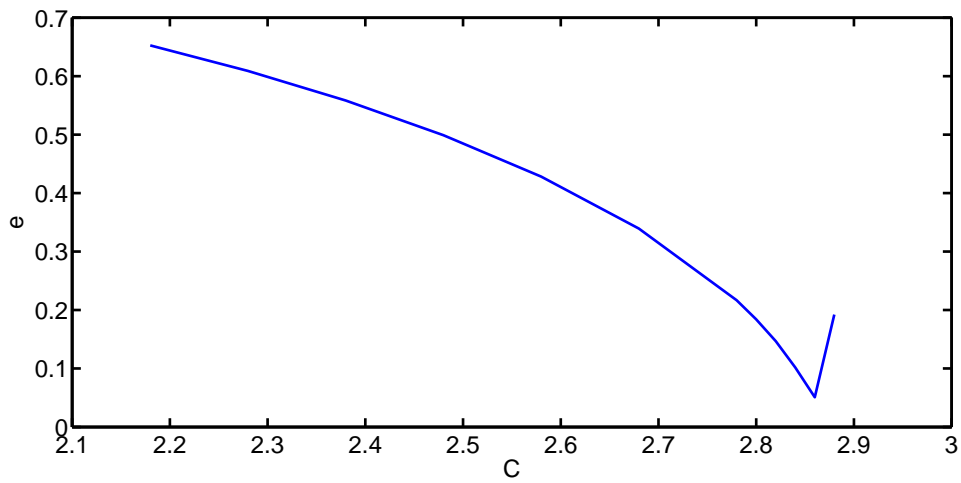


Figure 2.45: Variation in eccentricity of Saturn centered periodic orbit for $q = 0.9345$.

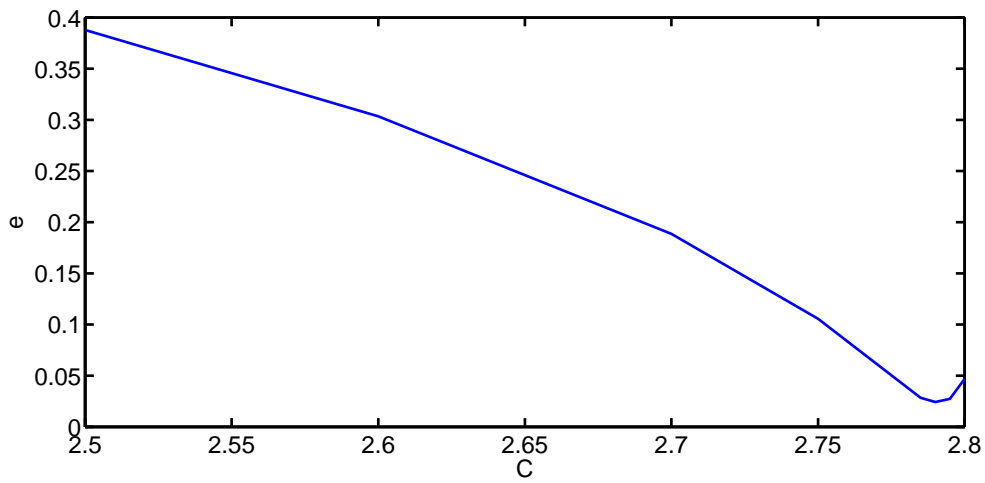


Figure 2.46: Variation in eccentricity of Saturn centered periodic orbit for $q = 0.9$.

for $C = 3.018$ it is 0.31045. It is the same C for which Figure 2.37 of semi-major axis has shown steep ascent of the curve.

Figure 2.43 shows the variation of eccentricity of Saturn centered periodic orbit for $q = 0.9845$. It is clear from figure 2.43 that as C increases, eccentricity decreases. But the steep ascent of the curve is observed between $C = 2.975$ and $C = 2.98$. For $C = 2.975, 2.98$ and 2.985 , the eccentricity takes values 0.1834, 0.2226 and 0.25884 respectively. It is for the same value of C for which Figure 2.38 shows the steep ascent of the curve in semi-major axis.

Figure 2.44 shows the variation of eccentricity of Saturn centered periodic orbit for $q = 0.9645$. It is clear from the graph that as C increases eccentricity decreases. But the steep ascent of the curve is observed between $C = 2.9$ and $C = 2.943$. For $C = 2.9$ eccentricity is 0.1376 and for $C = 2.943$ it is 0.2051. As earlier, it is same value of C for which Figure 2.39 shows the steep ascent of the curve in semi-major axis.

Figure 2.45 shows the variation of eccentricity of Saturn centered periodic orbit for $q = 0.9345$. It is clear from the graph that as C increases eccentricity decreases. Figure 2.46 shows the variation of eccentricity of Saturn centered periodic orbit for $q = 0.9$. It is clear from the graph that when C increases eccentricity decreases. But in this case the steep ascent of the curve in the graph occurs between $C = 2.795$ and $C = 2.8$. For $C = 2.795$ eccentricity is 0.0274 and for $C = 2.8$ it is 0.0469. It is for the same value of C for which Figure 2.41 showed the steep ascent of the curve in semi-major axis.

From Figures 2.42–2.46, it is concluded that as q moves from 1 to 0.9, eccentricity of Saturn centered periodic orbits decrease slowly up to certain limit of C and then increases. It means perturbation due solar radiation pressure slows down the tendency of quick change in semi-major axis and eccentricity against C .

2.3 Conclusion

From the analysis of PSS incorporating solar radiation pressure and oblateness as perturbing forces, it is observed that as the C increases, the number of islands, number of quasi periodic orbits and number of periodic orbits increases for any perturbation due to solar radiation pressure. As q tends to 1, admissible range of C increases. In other words, solar radiation pressure reduces admissible range of C . For $q = 1$ maximum value of C is 3.018. By increasing perturbation due to solar radiation pressure up to $q = 0.9845$ maximum value of Jacobi constant reaches $C = 2.985$, by increasing more perturbation due to solar radiation pressure up to $q = 0.9645$ maximum value of C decreases and reach at $C = 2.943$. For $q = 0.9345$, maximum value of C reaches at $C = 2.88$ and for $q = 0.9$ maximum value of C is 2.807.

It is further noticed that as C increases Sun centered periodic orbit and Saturn centered periodic orbits shift towards Saturn for a given perturbation due to solar radiation pressure q . It means Jacobi constant C acting opposite to gravitational force. For a given C , as q tends to 1, location of Sun centered and Saturn centered periodic orbits move towards Sun. That is solar radiation pressure is responsible for the shifting of periodic orbits towards Saturn which is expected as solar radiation pressure is opposite to gravitational attraction of Sun. Thus, by decreasing perturbation due to solar radiation pressure, effect of gravitational attraction increases and as a result periodic orbit shifts towards Sun. For a given q , as C increases semi-major axis increases and eccentricity of Sun centered periodic orbit decreases. For a given q and its corresponding maximum value of Jacobi constant C Saturn centered periodic orbit showing steep ascent of the curve in semi-major axis and eccentricity in certain subinterval of C .

It is observed that semi-major axis increases uniformly up to certain value of C and then shows a sharp increase, where as eccentricity decreases uniformly up to certain value of C and then shows a sharp increase. When the solar radiation pressure q tends to 0.9, this sharp change in the semi-major axis and eccentricity graphs becomes smooth. Thus, it is concluded that perturbation due to solar radiation pressure reduces steep ascent of the curve in semi-major axis and eccentricity of Saturn centered periodic orbits. It is further observed that as q tends to 1, semi-major axis and eccentricity of Sun centered periodic orbit increases for given C . In

other words, due to solar radiation pressure, semi-major axis and eccentricity of Sun centered periodic orbit reduces.